BOOSTER II

A 500 MeV BOOSTER INJECTOR FOR THE ZERO GRADIENT SYNCHROTRON

- A DESIGN REPORT

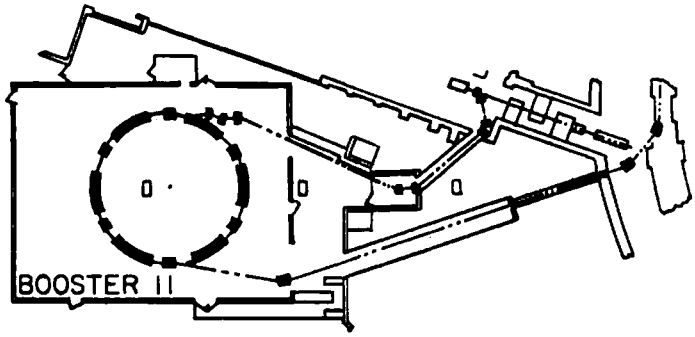

DRAFT

May 1975

D. Hardek

- FOREWORD -

This report summarizes major design considerations for the 500 MeV booster injector now under construction by the Accelerator Research Facilities Division. It is the first such document for general distribution. As designs are refined, some changes are expected and updated versions of this report or parts thereof may be distributed.

A large number of people have contributed to designs presented here--they will not be individually listed. It will be by their talents and continued effort that the booster project will be a success.

James D. Simpson

TABLE OF CONTENTS

Table of Contents (continued)

LIST OF FIGURES

LIST OF TABLES

I. Introduction

A. Background

All major proton accelerators have recognized the need for and have implemented intensity improvement programs during recent years. As a result of accommodation of more simultaneous beam users and/or requirements of higher beam intensities to conduct competitive physics programs, the improvement efforts have universally sought to increase the injection energy to the accelerators. This follows from the energy dependence of the space charge limit (the limiting factor in most cases) which is proportional to $\beta^2 \gamma^3$.

The possibilities and advantages of higher injection energy for the ZGS were studied as early as 1966. At that time, a joint study with MURA[1] investigated high energy injectors. That study showed a 200 MeV linac to be the most straightforward approach (later adopted by BNL and the Fermi National Accelerator Laboratory). It also pointed out that a rapid cycling synchrotron "booster" would be considerably less expensive than a linac, but that the problem of injecting enough protons into a small synchrotron to produce usable intensity was serious.

B. ZGS Booster Injection Program

As H^- ion source technology improved, it became evident that the solution to the injection problem in a booster synchrotron was solvable by using "stripping injection". This scheme, in which H^- ions are injected into closed orbits and then stripped to protons,

permits many turns to be injected into the same transverse phase space area.[2] While the principle involved was straightforward, there were several problem areas. These included development of suitable stripping techniques and equipment and development and construction of an operationally reliable, high current H^- ion source.

The 2.2 GeV electron synchrotron at Cornell University was brought to Argonne in 1969 when it was excessed by Cornell. At Argonne, the machine was provided new vacuum chambers, accelerating systems, diagnostics, extraction system, and stripping injector equipment. The modified machine was renamed BST-I and served as a valuable tool in the development of the techniques mentioned above.

The achievements of BST-I have been significant not only to the ZGS program, but also for accelerator technology in general. Stripping injection has been shown[3] to be a practical alternative method offering potentially better operation for most synchrotrons. Tests have resulted in circulating beam "brightness" a hundred times that of the injected beam, and 180 turns injected into a machine whose acceptance was less than 4 times the injected emittance. An operational, high intensity (16 mA peak, 500 μsec long) rapid cycling H^- ion source was developed.[4] It is, at this time, the only known source with these characteristics which is suitable for use with a linac. Finally, the 40 $\mu g/cm^2$ foils required for stripping injection and the handling mechanism for them have been realized. Tests with BST-I used foils for over 10^7 injection pulses each, with several

foils experiencing more than 5×10^{19} proton traversals/cm^2 (at 50 MeV) before mechanical failure. A summary of BST-I accomplishments and valuable experience includes:

1. Development of techniques and equipment to make H^- injection a practical method.
2. Demonstration of brightness increase ~100X in orbiting beam compared to injected beam.
3. Experience with the design, construction, and operation of single turn extraction equipment (e.g., fast kickers).
4. Experience with various accelerating techniques (e.g., rf capture, diagnostics) employed in rapid cycling machines.
5. Experience with operating characteristics of strong focusing synchrotrons.

As a result of the accomplishments of BST-I and the availability of funding, effort has been directed toward the design, construction, and operation of a 500 MeV injector synchrotron for the ZGS. The new machine, BST-II, is designed to accelerate $>3 \times 10^{12}$ protons per pulse. With a beam transfer system designed to stack up to eight such pulses in the ZGS, it will be possible to achieve ZGS intensities of several times 10^{13} protons. Aside from possible unanticipated new beam instabilities associated with high intensity ZGS operation, the first known limiting factor will be the effects of beam loading on the ZGS rf system. Calculations predict possible rf problems at intensities of $>10^{13}$ protons.

In addition to providing 500 MeV protons for the ZGS, the beam

may also be used for medical applications (radiography and therapy) and for the production of pulsed neutrons for solid state physics applications.[5] This report provides information concerning design characteristics of BST-II.

References

1. Study of High Intensity Injectors for the ZGS, Midwest High Energy Study Group, 1966.
2. G. I. Dimov, et al., USSR National Conference on Particle Accelerators, Moscow, USSR, October, 1968.
3. J. D. Simpson, "Operating Results from the ANL Booster," Proceedings of the 1973 Particle Accelerator Conference, San Francisco, California, March, 1973.
4. J. A. Fasolo, "A High Intensity H^- Source for Injection into Proton Synchrotrons," Proceedings of the Second Symposium on Ion Sources and Formation of Ion Beams, Berkeley, California, October, 1974.
5. "Applications of a Pulsed Spallation Neutron Source," Report of a Workshop held at Argonne National Laboratory, May, 1973, ANL-8032.

II. Machine Design

A. Constraints Influencing Design

The important criteria and constraints influencing the design of Booster-II were set as:

1. The circumference ratio (ZGS/BST) must be an integral number in order to simplify beam transfer.
2. The space charge limit must be high ($>5 \times 10^{12}$ at 50 MeV). An accelerated intensity of at least 3×10^{12} protons has been assumed in determining the requirements for apertures, and for injection and rf systems.
3. The design must permit H^- injection and subsequent stripping.
4. Adequate straight sections must be provided for the accelerating cavities, correction devices, diagnostic, and extraction equipment.
5. The magnet design must allow for possible 60 Hz operation even though it will initially operate at 30 Hz (refer to Section I, Reference No. 2).
6. The transition energy must be as high as possible, preferably $\gamma_{tr} = 2$ or more. This avoids accelerating through transition energy and is high enough above γ (500 MeV) to facilitate synchrotron matching between the ZGS and the booster.
7. Cost must be minimal, since the project is funded from Accelerator Improvement monies.

B. Lattice

1. Configuration

A number of possible lattice configurations were examined. It was desired that there be long enough straight sections for extraction magnets and accelerating cavities without extra quadrupoles for matching. A transition energy greater than two required that the number of periods be greater than four. Ultimately, a machine with six periods of DOOFDFO was selected as best satisfying the requirements of Section II A. Each period contains two types of magnets: A short D magnet and a long FDF triplet. One D magnet is used to bend the incoming H^- beam to coincide with the closed orbit. Another D magnet, following the second extraction kicker, helps to bend the extracted beam into a septum magnet in the next long straight section. RF cavities occupy two of the long straight sections. The machine layout is shown in Fig. 1 and the dimensions and other parameters are shown in Table 1. The β-function and the momentum error function are shown in Fig. 2. Since the tune changes that can be provided using quadrupoles are proportional to β, the differences in the horizontal and vertical β-functions at the ends of the straight section can be used to decouple the corresponding tune changes. These locations are also to be used for orbit and midplane correcting dipoles and for sextupoles to correct for momentum-dependent tune changes.

The shapes of the β functions were also adjusted to use efficiently the "good" field volume of the ring magnets. This is shown in Fig. 3 where the maximum absolute X is plotted against the maximum absolute Y at injection through one period. (The maximum X includes an assumed momentum error of $\pm$ 0.4% $\Delta p/p$.)

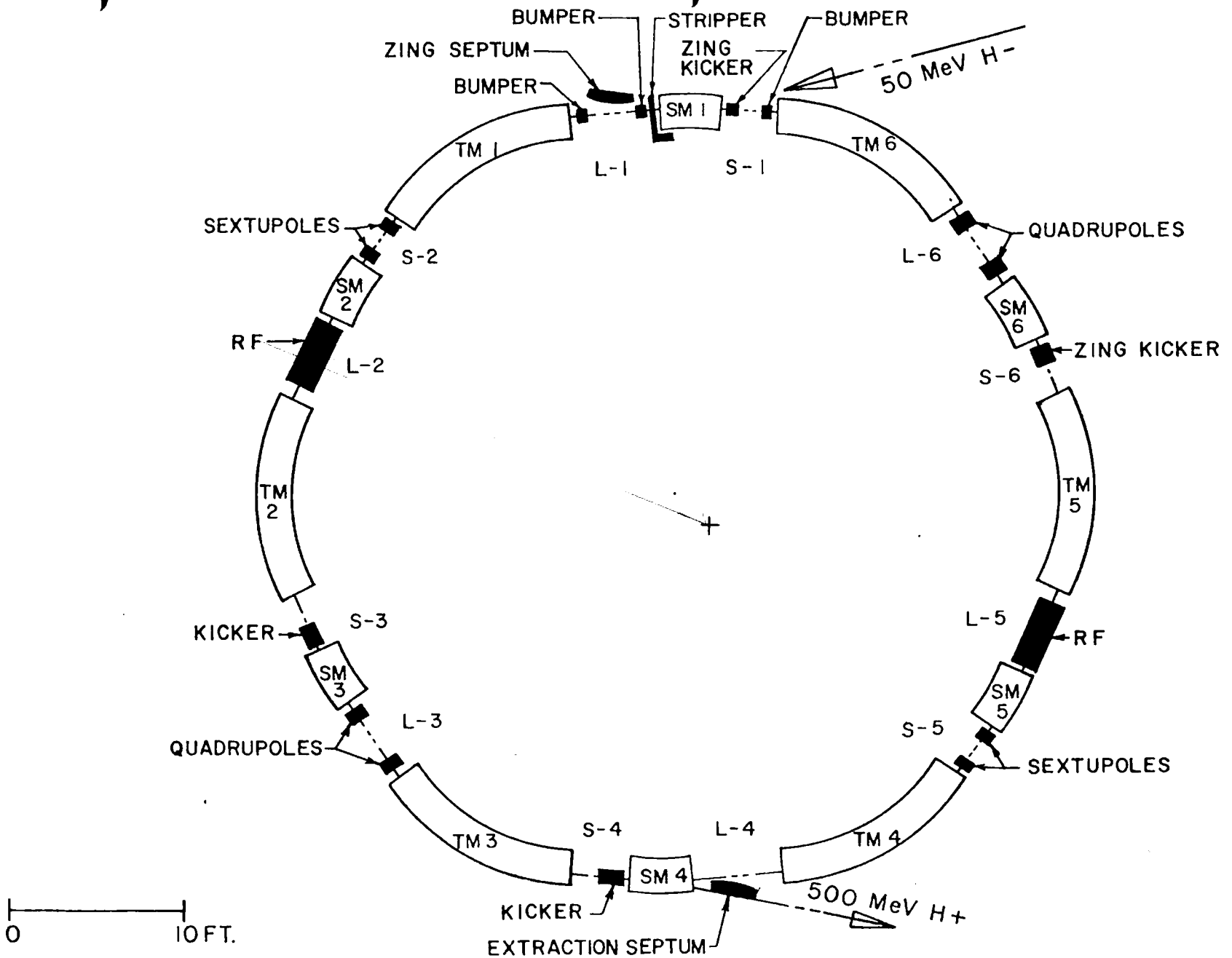

FIG. 1 BOOSTER II MACHINE LAYOUT

TABLE I

MACHINE PARAMETERS

Circumference	1691.06 in.
Average radius	269.14 in.
Circumference ratio ZGS/booster	4
Number of periods	6
Structure	DOOFDFO
Short straight section	54 in.
Defocusing magnet	26.151 in.
Long straight section	76 in.
Triplet magnet section	125.692 in.
F magnet near long section	34.458 in.
D magnet	54.724 in.
F magnet near short section	36.510 in.
Magnet radius	145 in.
Normalized gradients	
At injection F	0.0811/in.
At injection D	0.0812/in.
At 500 MeV, F	0.0810/in.
Central gap	2.46 in.
Height for good field region	2 in.
Width of good field region	4 in.
Field at 50 MeV (injection)	2.81 kG
RF frequency at 50 MeV	2.91 MHz

TABLE I (continued)

RF frequency at 500 MeV	5.29 MHz
Harmonic number	1
ν_x	2.2
ν_y	2.32
B_x	50-275 in.
B_y	68-211 in.
Displacement due to momentum error	50-82 $\frac{\Delta p}{p}$ in.
X quality for filled chamber at injection	8.2 π mrad in.
Y quality for filled chamber at injection	5.0 π mrad in.
Tune change per 10^{12} protons	$\Delta \nu_x$ -0.0087
	$\Delta \nu_y$ -0.0121

γ extraction

γ_{TR} =

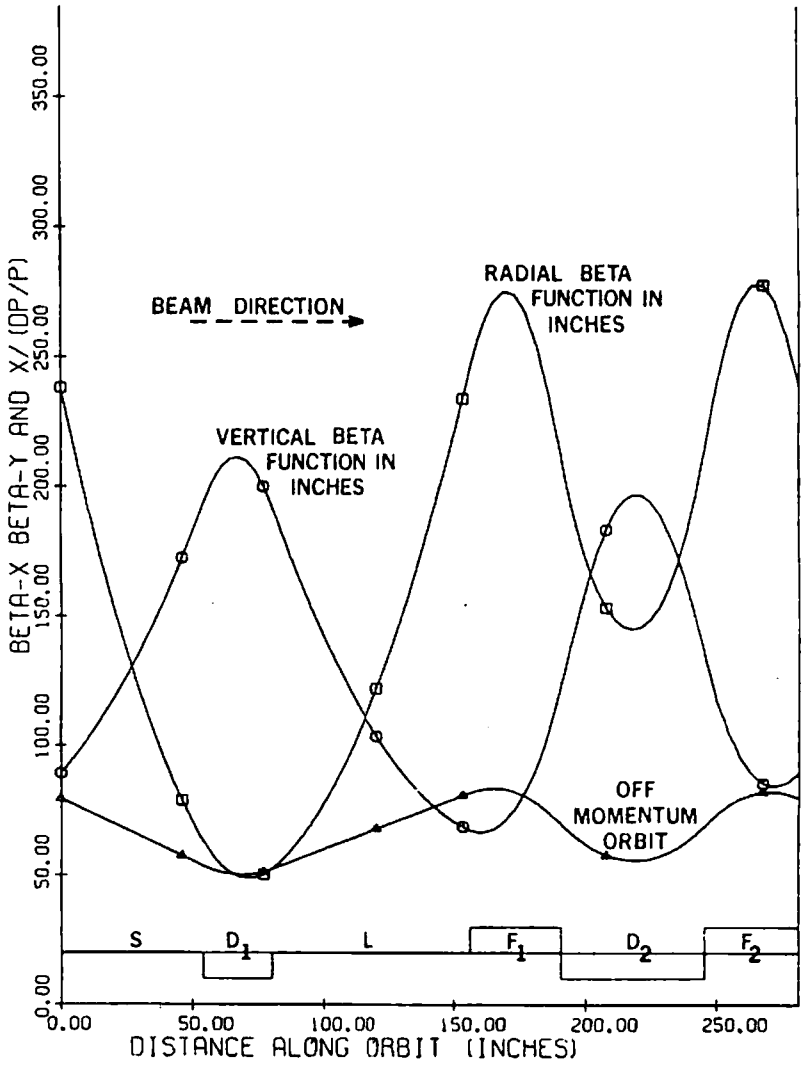

FIG. 2 BOOSTER II LATTICE FUNCTIONS

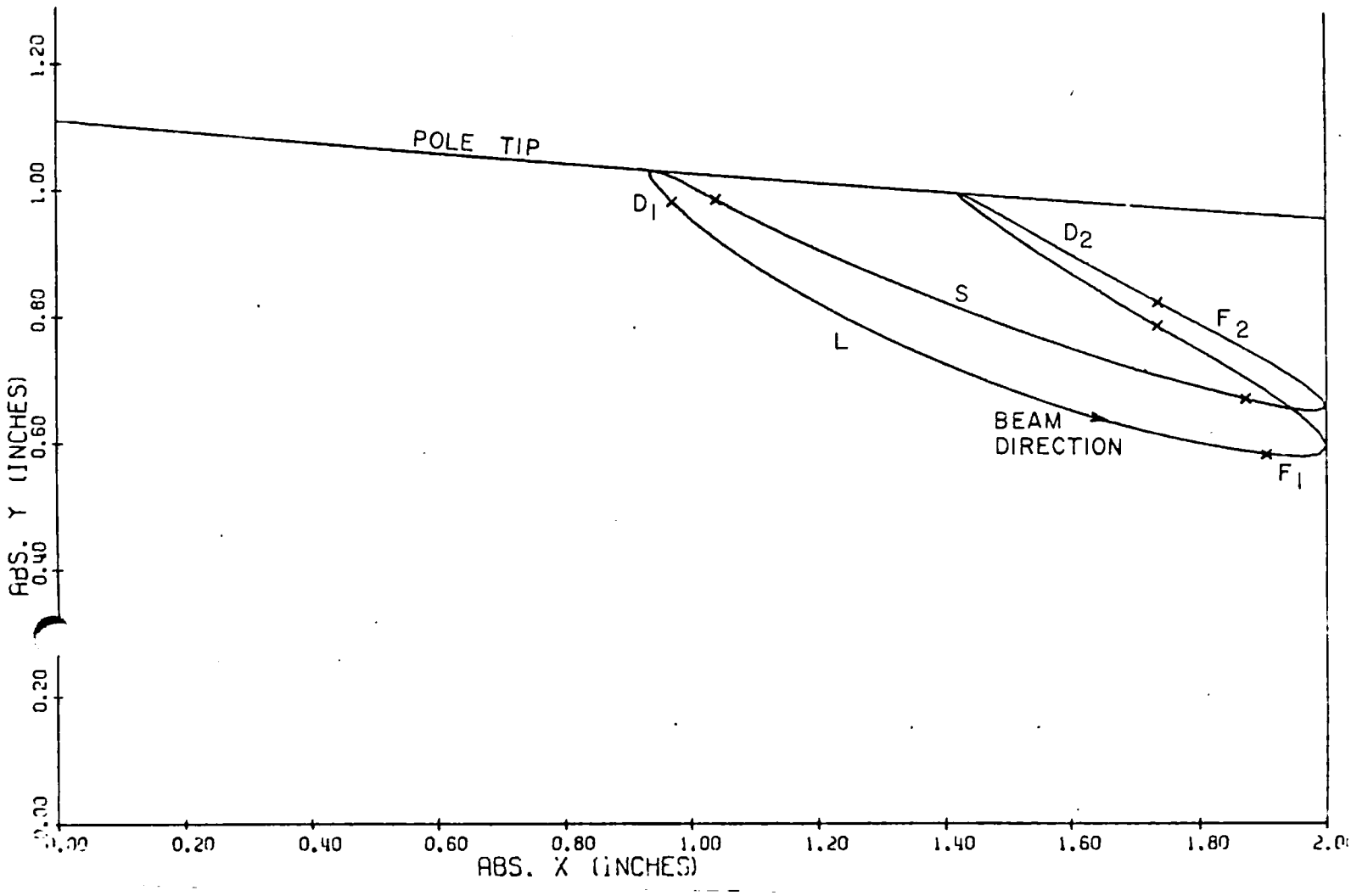

FIG. 3 MAXIMUM |X| vs MAXIMUM |Y| THROUGH ONE PERIOD OF BOOSTER II

2. Main Ring Magnets

The main magnets for the Booster II ring consist of two types, a D-type singlet and an FDF triplet. The only structural differences between these two types are the laminated core lengths and the make up of the core lamination geometry (F or D) used. The core steel consists of M45, CRFP nonoriented electrical steel from United States Steel and is 0.014 in. thick. This sheet material contains an AISI type C5 inorganic insulation on both surfaces. The laminations made from this material are one piece, having no midplane separations.

The cores are stacked on a radius of 145 in. at the gap centerline. This is done by allowing the laminations to fan out radially. Inserts of partial laminations or nonmagnetic filler inserted from the outer radius edge of the core maintain the desired magnetic steel density distribution.

Stainless steel (SST) keys are welded under tension between 1 in. thick SST plates at each end of the core. The laminations are also welded to these keys. The remaining magnet design is similar to that used for the booster magnets at the Fermi National Accelerator Lab.[1] The laminated core and coil are located inside a vacuum tight stainless steel housing with four penetrations for the coil leads located on the inside radius surface. The entire volume inside this housing except for the magnet gap and the volume between the upper and lower coils is vacuum impregnated with an epoxy having high radiation resistance and low vacuum outgassing. This permits operation of each magnet as part of the high vacuum system of the ring without requiring a vacuum chamber to be placed inside the magnet gap.

A typical cross section through a magnet is shown in Fig. 4.

The coil design for the main ring magnets has calculated operating parameters that are within certain limits defined by the power supply, the power distribution system, the cooling water system, and the magnitude of acceptable eddy current losses in the coil conductors. The resulting coil is made from OFHC hollow copper conductors with 0.289 in. square cross section. The electrical circuit of the coil in each magnet consists of two series connected groups of 9 parallel connected pieces of conductor. There are 14 turns around the poles of each of the 12 magnets in the ring with a current of 2500 A_{rms} at the terminals of each magnet. All magnets in the ring are then electrically connected in series. The locations of the conductors in the coil pack are chosen to provide a uniform flux linkage and a uniform resistance for each of the 18 conductor circuits.

Structural and operating parameters for the magnets are indicated in Table II.

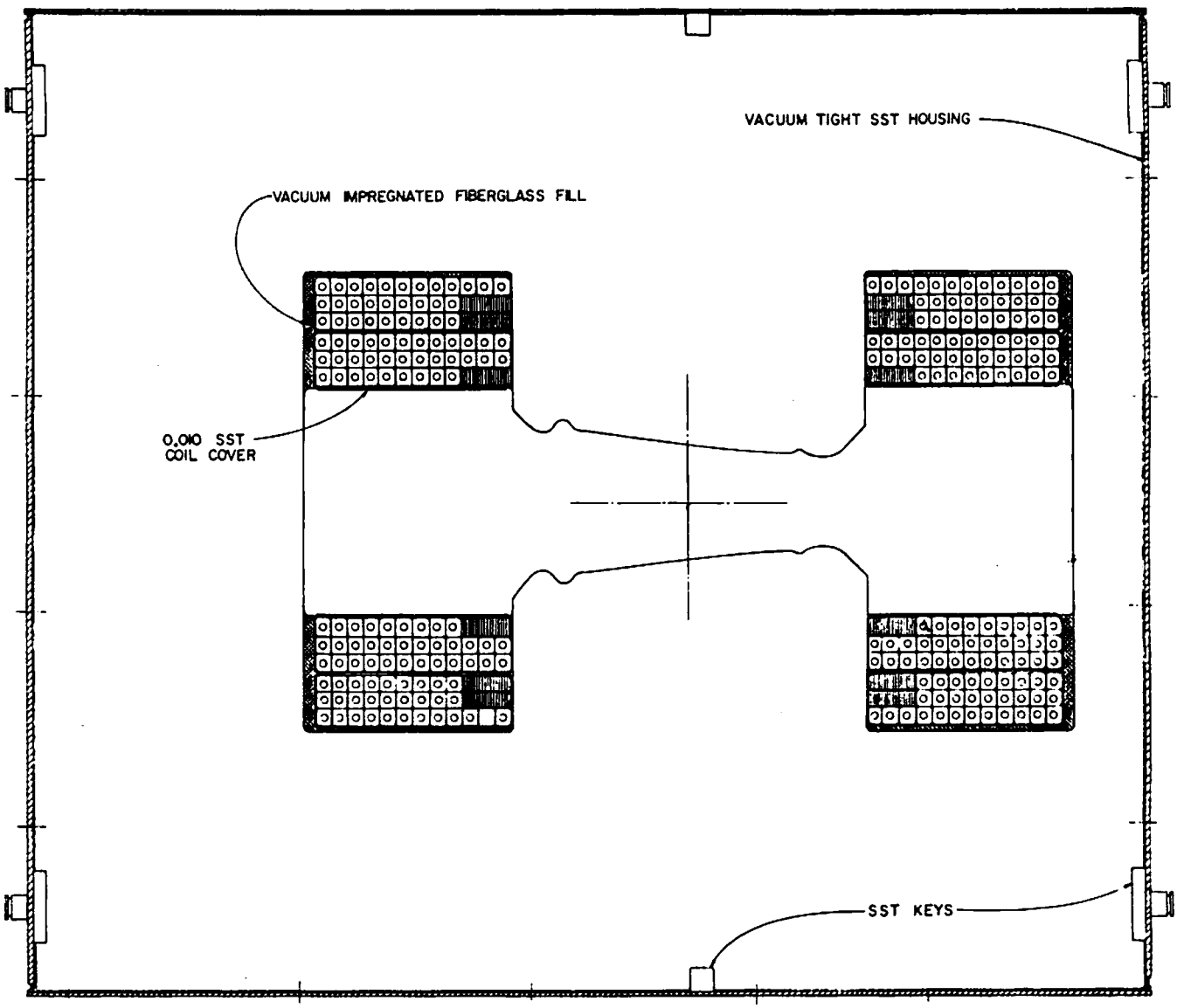

FIG. 4 TYPICAL RING MAGNET CROSS SECTION

Table II

PARAMETERS FOR THE BOOSTER II MAIN RING MAGNETS

F-Laminations, Weight	41,658 lbs (total weight)
D-Laminations, Weight	46,074 lbs (total weight)
Excitation Frequency	60 Hz (max)
DC Ampere-Turns	31934
AC Ampere-Turns (Max.)	17782
RMS Ampere-Turns	34321
Resistance	0.0444 ohm
Inductance	23.5 H
Conductor Size	0.289 $in.^2$ x 0.161
Conductor Weight	5550 lbs
Current Density	4600 $A_{rms}/in.^2$
Power Dissipation ($I^2_{rms}R$)	267 kW
Core Losses (Using 0.5 Watts/lb)	44 kW
Coil Eddy Current Losses	27 kW
Maximum Stored Energy	143.7 kJ
Coolant Water Pressure Gradient	120 psi
Coolant Flow for a $30^{\circ}F$ ΔT	67 gpm

Upon receipt of the first singlet and first triplet magnets, detailed measurements of the structural and operating parameters will be made. First conformity of structural dimensions to design values will be verified. The integrity of the cooling and electrical circuits in each magnet will then be established. This will be done by measuring the resistance and inductance of each magnet and finding the water flow as a function of the pressure gradient across the cooling circuits. The insulation between the coil conductors and the magnet core will be tested with a 1000 V dc megger.

With these measurements successfully completed, each magnet will be energized. First, direct current will be supplied and the magnetic field at several locations in the gap will be measured using flip coils and electronic integrators. Several currents between the value at injection and the RMS value will be selected. At each setting the temperature gradient across each water circuit will be determined to further verify coil integrity. At both the injection and RMS values, transverse scans will be performed at various vertical locations in a defocusing gap and a focusing gap. These results will provide useful comparisons with the calculated values of the central field, the field gradient, and the sextupole component of the field. The first singlet will also be measured, point by point, through the entire gap using a digitally controlled manipulator to position a small search coil. This data will provide information on the effective length of the field and the integrated field as a function of the position across

the gap. These results will then be used to calibrate long, curved, printed-circuit coils that will be used in the measurements of the remaining magnets.

After the dc field measurements are completed, the magnets will be energized with 60 Hz alternating current. Measurements similar to those done for the dc excitation will be repeated. In addition, measurements of the integrated field across the gap will be made using curved, flat, printed circuit coils that extend through the entire gap of each magnet. This will provide information on core loses and on the effects on the gap fields due to the eddy currents in the cores and coils.

After tests on the first singlet and triplet magnets have been completed they will be used as reference magnets for comparison with the succeeding magnets. The next two of each type will be compared in detail using automated manipulators to position search coils in the gaps. Both dc and ac comparisons will be made. Direct comparison will also be made with alternating current by placing flat printed-circuit search coils through the gaps of the reference magnet and the magnet under test. The two magnets will be powered in series and the search coils will be connected so the outputs cancel resulting in a signal that is proportional to the differences between the two magnets. If this comparison proves to be consistent with that resulting from the point by point data, this method of comparison will be used on the remaining magnets. If not, the point by point method will be used throughout.

The first three magnets of each type to be tested will show how the parameters fluctuate from magnet to magnet in the actual fabricating process. At this time it will be decided if these differences are small

enough to disregard. In this case, installation of the magnets can begin. If differences are too large, all magnets may have to be received and tested before installation can begin. Details on criteria for this decision will be made as measurement data becomes available.

---

[1] R. Billings, W. Hanson, P. Reardon, "The NAL Booster Magnets," The Third International Conference on Magnet Technology, Hamburg, 1970, Page 537.

3. Resonances Near the Operating Points

The location of the operating points and some possible low order resonances are shown in Fig. 5. It can be seen that there is enough operating area to provide for the expected tune change for up to 10^{13} protons per pulse at 50 MeV. If the two sextupole error resonances near the operating line prove to be troublesome, the tunes can be shifted to larger υ_x and smaller υ_y using correcting quadrupoles. In any event, the correcting quadrupoles can be used to study the effects of these resonances during the tune up period of the machine.

4. Corrections

a. Tunes

The tune change produced by a single quadrupole placed anywhere around the machine is given by

$$\frac{\Delta \nu}{\Delta Q} = \frac{\beta}{4\pi B\rho}$$

where β is the beta function value at the quadrupole, $B\rho$ is the proton rigidity, and ΔQ is the quadrupole gradient times the length. A positive sign for ΔQ denotes focusing.

Since the β-functions for the horizontal and vertical envelopes are different at each end of the straight sections, quadrupoles placed there are used to position the operating point. Short

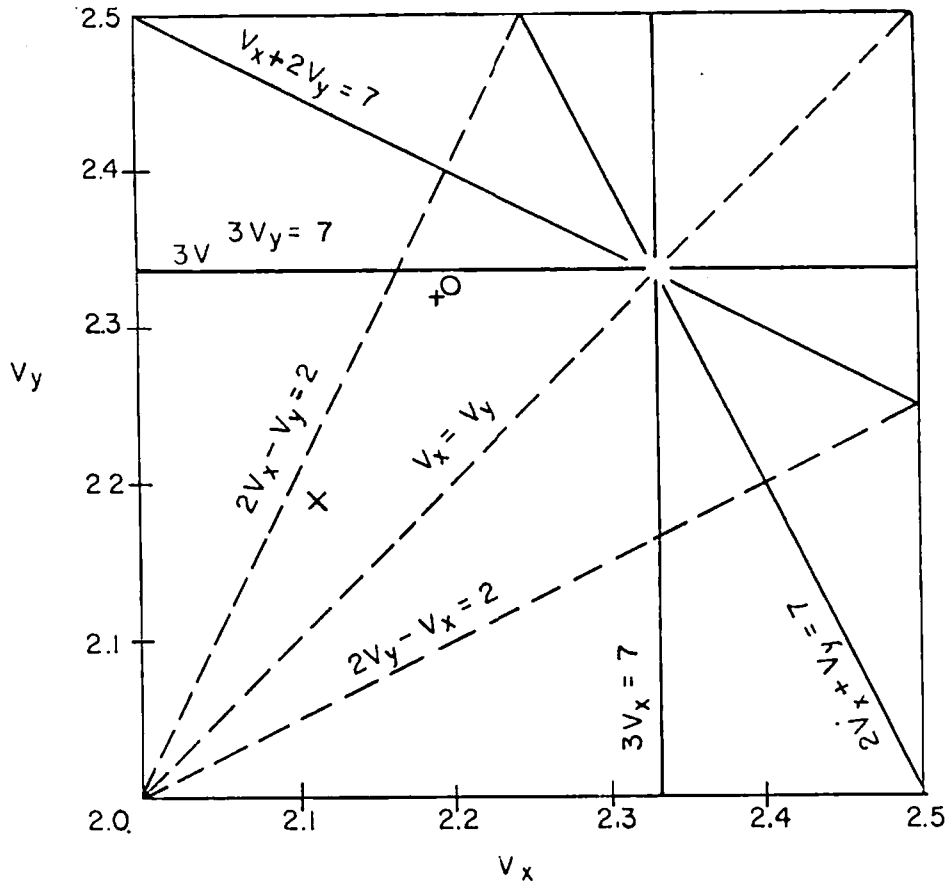

--- COUPLING RESISTANCE
O OPERATING POINT, INJECTION
\+ OPERATING POINT, EXTRACTION
× OPERATING POINT, 10^{13} 50 MeV PROTONS

FIG. 5 RESONANCES NEAR OPERATING POINT

quadrupoles centered 9 in. from the magnet in one long straight section give the following results (at 50 MeV).

$$\frac{\delta \nu_x}{\delta Q} = 0.0124 \text{ upstream}$$

$$\frac{\delta \nu_x}{\delta Q} = 0.0432 \text{ downstream}$$

$$\frac{\delta \nu_y}{\delta Q} = -0.0311 \text{ upstream}$$

$$\frac{\delta \nu_y}{\delta Q} = -0.0138 \text{ downstream}$$

(Q units kG in. /in.

"Diagonalization" gives

Tune shift	Q upstream	Q downstream
$\Delta \nu_x = 0.1 \quad \Delta \nu_y = 0.0$	-1.18	2.65
$\Delta \nu_x = 0.0 \quad \Delta \nu_y = 0.1$	-3.68	1.06

b. Chromaticity

In general, momentum errors in a strong focusing accelerator lead to tune changes given by the expression

$$\frac{\delta \nu}{\nu} \approx \frac{\Delta p}{p}$$

The cylindrical design of the Booster II focusing and defocusing magnets provides sextupole terms that tend to reduce this effect. This can be shown as follows.

The scaler potential used for the magnet design,

$$v = B_o \left\{ (1 + n)\, y - \frac{n}{R} \left[3\, y \sqrt{r^2 + y^2} + (r^2 - 2\, y^2) \sinh^{-1} \frac{y}{r} \right] \right\},$$

gives the following equations of motion (to second order in $s = r - R$, and y).

$$x'' + x\,(1 - n) = \frac{n}{R} \left(x^2 - \frac{y^2}{2} \right)$$

$$y'' + y\, n = - \frac{n\, x\, y}{R}$$

If one adds a momentum error and expands about the new equilibrium orbit, x_p, the linear oscillation equations become

$$x'' + x \left[(1-n)\left(1 - \frac{\Delta p}{p}\right) - \frac{2n\, x_p}{R} \right] = 0$$

$$y'' + y_n \left(1 - \frac{\Delta p}{p} + \frac{x_p}{R}\right) = 0$$

In Booster II, $\frac{x_p}{R}$ is as large as $1/2 \frac{\Delta p}{p}$.

Without taking this compensation into account, a 1% momentum error in Booster II produces tune changes of

$$\Delta \nu_x = - 0.0274, \quad \Delta \nu_y = - 0.0225$$

The quadrupole strengths in one long straight section needed to correct these tune shifts are as follows: (see 4a)

$$Q = - 1.151 \text{ kG in./in. (upstream)}$$

$$Q = + 0.965 \text{ kG in./in. (downstream)}$$

Since both the tune shifts and orbit positions are proportional to the momentum error, these chromaticity tune shifts are compensated by using sextupole magnets in the same locations. For a 1% momentum error, the orbit positions are respectively, 0.56 in. and 0.78 in. at the upstream and downstream long straight section positions. Therefore, the required sextupole strengths are given by:

$$S = \frac{-1.151}{0.56} = - 2.06 \text{ kG in./in. (upstream)}$$

$$S = \frac{0.965}{0.78} = 1.24 \text{ kG in./in. (downstream)}$$

To avoid unnecessary broadening of the third order, seventh harmonic resonances near the operating point, the corrections are placed so as to provide only even harmonics. Two diagonal straight sections are used.

C. Correction Magnets

The Booster II tune correction magnets consist of two types: quadrupole and sextupole. Four quadrupole magnets are located at the upstream and downstream ends of both the L3 and L6 straight sections. Four sextupole magnets are similarly located in the S2 and S5 straight sections.

The cores of all correction magnets consist of M22, CRFP nonoriented electrical steel, 0.025 in. thick, with AISI-C4 core plate insulation on both sides. Each core is made from either four or six identical pole sections which are stacked to a height of 6.125 in. There is a 1/4 in. stainless steel (SST) plate on each end of each core stack. Threaded tie rods extend through each core and end plate to provide an average core compression of 60 psi.

The coils for each magnet are made from OFHC hollow copper conductor, 0.230 $in.^2$. After the coils are installed in the core stack, the magnet assembly is placed inside a vacuum tight SST housing. The core, coils, and all voids inside the housing but outside the magnet bore are filled by vacuum impregnation with an epoxy resin having high radiation resistance and low vacuum outgassing. The impregnation of the bore of each magnet is prevented by inserting an inflatable bag into the bore during this process. This technique is similar to that used to fabricate the main magnets.

The magnets are mounted inside of 24 in. o.d. SST pipe in their corresponding straight sections. Each is attached to an independently

adjustable support and is positioned so that the center of each is on the axis of the pipe. Water and power are fed to the magnets through insulated feedthroughs in the wall of the vacuum pipe.

Four programmable power supplies are required to excite the eight correction magnets. One powers the quadruple magnets in the upstream locations in the two associated straight sections; similarly one power the two downstream magnets. Each pair of magnets is electrically connected in series. The sextupole magnets are powered in a like manner.

The structural and operating parameters for the correction magnets are indicated in Table III.

Table III

Parameters for Booster II Correction Magnets

	Quadrupole	Sextupole
Overall Length (in.)	9-3/4	8-3/4
Bore Diameter (in.)	5.0	5.0
Sectional Diameter Over Flats (in.)	16	13
Max. Field at Pole (kG)	15.7	10.9
Max. Integral Gradient	$19\left[\frac{kG}{in.} - in.\right]$	$11.2\left[\frac{kG}{in.^2} - in.\right]$
Max. Ampere Turns/Pole (kA)	17.8	8.9
Maximum Current (A)	635	635
Maximum Voltage (Volts)	34.8	25.0
Power Dissipation (kW)	22.1	15.9
Number of Water Circuits/Pole	2	1
Coolant Water Pressure Gradient (psi)	126	112
Coolant Flow for $30^{\circ}F$ ΔT(gpm)	5.1	3.6

C. Injection

1. Technique

As stated earlier in this report, H^- ion stripping injection is employed in BST-II in order to achieve the designed intensity. Very briefly, H^- stripping injection's advantage is that the statistical nature of the stripping process permits incoming beam to be injected into the same phase space as recirculating beam without the usual constant phase space density limitation. In principle, the brightness which can be achieved is limited only by dilution caused by scattering of beam in the stripper and by machine limitations.

In order to reach designed intensities in BST-II, it is necessary to fill the transverse acceptances of the machine as uniformly as possible. In the vertical plane, scattering by the stripping foil accomplishes this, but other techniques are required to fill the larger, horizontal acceptance.

Three alternative techniques were examined:

a. Injecting to a moving stripper as it sweeps the horizontal aperture, using small steering magnets in the 50 MeV beam transport to "track" the stripper. The stripper in this case would be mounted on the perimeter of a rotating wheel, similar to the design used in BST-II. Schemes were examined in which stripping occurred following both F-(in triplet) and D-type ring magnets.

The main disadvantages of this method are the high vacuum load produced by the large wheel housing, timing jitter problems,

and the relatively complicated mechanical systems required. On the other hand, techniques were reasonably well developed in BST-I, and some of the BST-I equipment could be reused.

b. Injecting, beginning almost a millisecond before minimum field, to a fixed stripper at an inside radius. As the magnetic field falls, the equilibrium orbit shifts outwards, thus filling progressively larger betatron amplitude phase space.

The advantage of this system lies in its simplicity, but the fact that the off-momentum condition forces the orbit "inside" in the "D" magnets of the triplets results in a reduction of vertical acceptance. Furthermore, at the time when one would want the circulating beam to move off the foil rapidly to minimize scattering dilution, $\dot{B}$ is diminishing.

c. Using small, pulsed, bump magnets, locally distort the orbit at the injection point. The incoming beam can be injected to a fixed stripper inside the normally used acceptance of the machine. The local closed orbit can than be moved from the stripper at a programmable rate.

After considering the pros and cons of the above cited schemes, that described in c was selected for use in BST-II. A descriptive diagram of the method is given in Fig. 6.

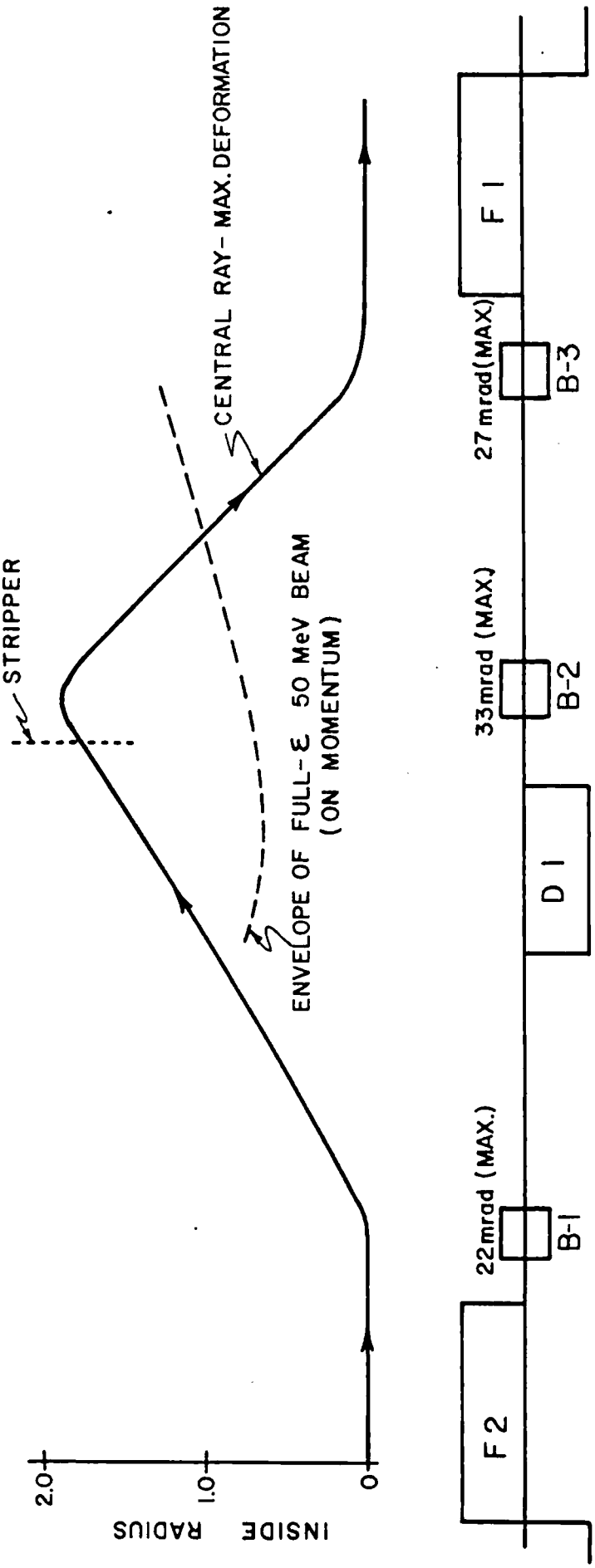

FIG. 6 DEFORMATION OF ORBIT FOR INJECTION

2. H^- Source Requirements

Phase space dilution due to scattering in the 40 [$\mu g/cm^2$] stripper foil is about 10^{-2} [mrad-in.] per pass. For most of the injection period, circulating beam passes through the foil about every other turn. These considerations together with a comparison of injected emittances and machine acceptances suggest an injection duration of 300-400 μsec. For 95% stripping efficiency, 90% matching efficiency, and 70% capture, the corresponding H^- currents at 50 MeV required for 5×10^{12} protons are 6.0 and 4.5 mA. A source development program to provide this capability has been funded and is underway.

3. Stripper Requirements

A fixed stripper mechanism must be constructed. Provisions for remote changing of foils will be provided. Conceptual designs operate on a principle similar to a slide projector tray. Each "slide" is a U-shaped frame holding a foil.

D. Extraction

Beam is extracted from Booster II in one turn using beam steering, two ferrite kicker magnets, and one septum magnet.

The beam will be steered outside of the central orbit so that beam center is at +0.6 in. at the exit from the singlet magnet D1. This places the beam near the septum of the extraction magnet.

The first kicker magnet will be located in the BS3 short straight section and will produce a 12 mrad inward kick. The second kicker will be located in the BS4 short straight section which is approximately one half betatron wavelength downstream from BS3. The kick in the second magnet is 15 mrad outward and effectively adds to the angle produced by the first kicker.

A horizontally defocusing magnet D1 is located between BS4 and the extraction septum magnet located in BL4. This D1 magnet produces an additional 12.7 mrad of bend.

The extraction septum magnet is pulsed to 1.0 T, is to 36 in. long, and is curved to follow the beam path.

The extraction scheme is shown in Fig. 7.

The fast extraction kickers is use Ceramil Magnetic's type C2050 ferrite. They are 27 in. long (22 in. effective magnetic length) and have a 2-in. by 4-in. gap. The $\int B \cdot dl$ for the kicker in S4 is 0.0436 T-M. The magnetic field required in the S4 kicker is 0.097. Each magnet has an inductance per unit length of 2.51×10^{-6} H/m

and is designed as a 22 ohm transmission line. Loading capacitances of 2840 pF are required to achieve the impedance. They are split into eleven discrete sections. The filling time of each is 63 nsec, leaving 31 nsec for rise time and jitter.

A line current and voltage of 4091 A and 91 kV is required to produce 0.097 T. The charging voltage is 182 kV. A schematic is shown in Fig. 8.

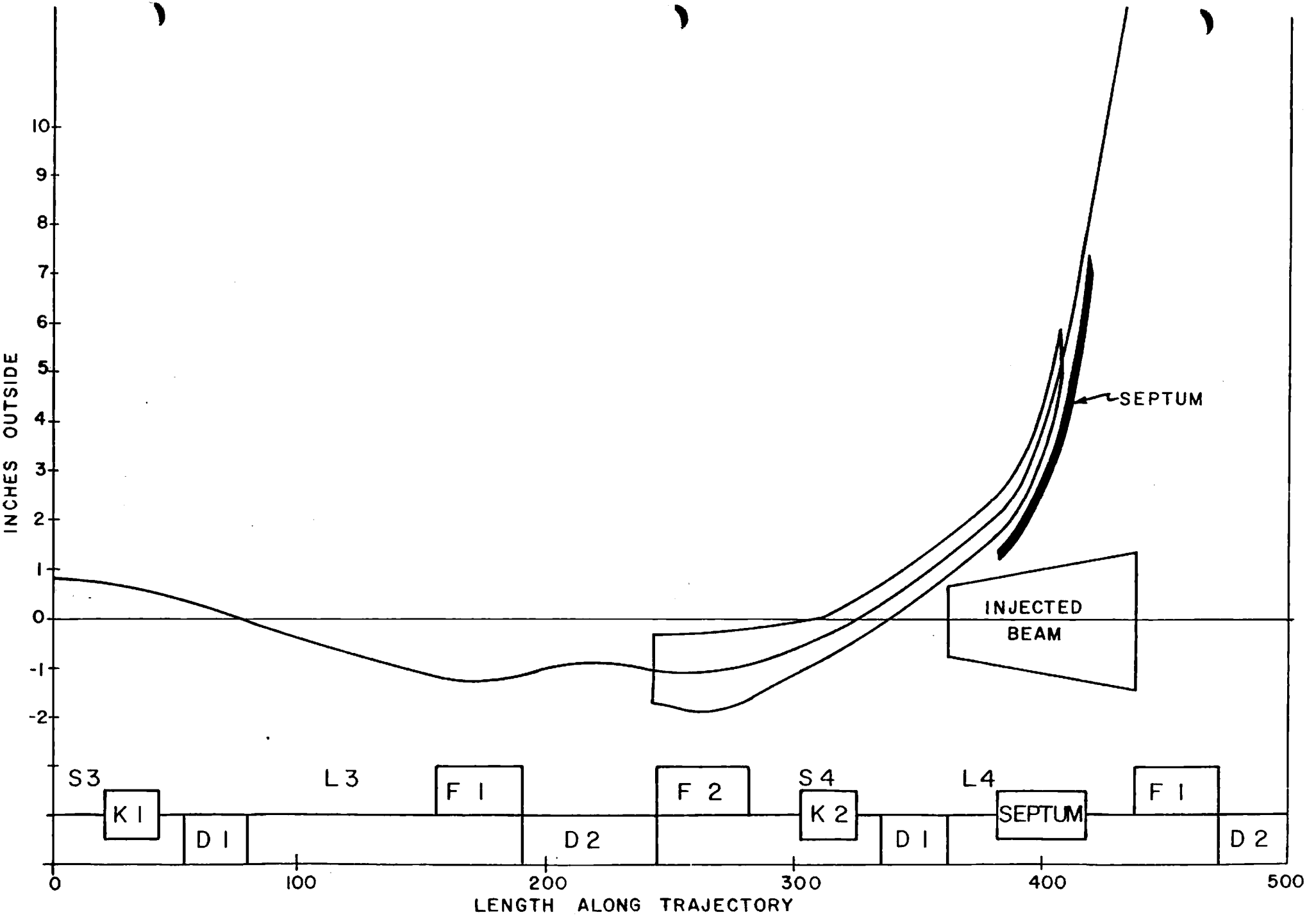

FIG. 7 EXTRACTION ORBIT

Charge and Discharge Circuit

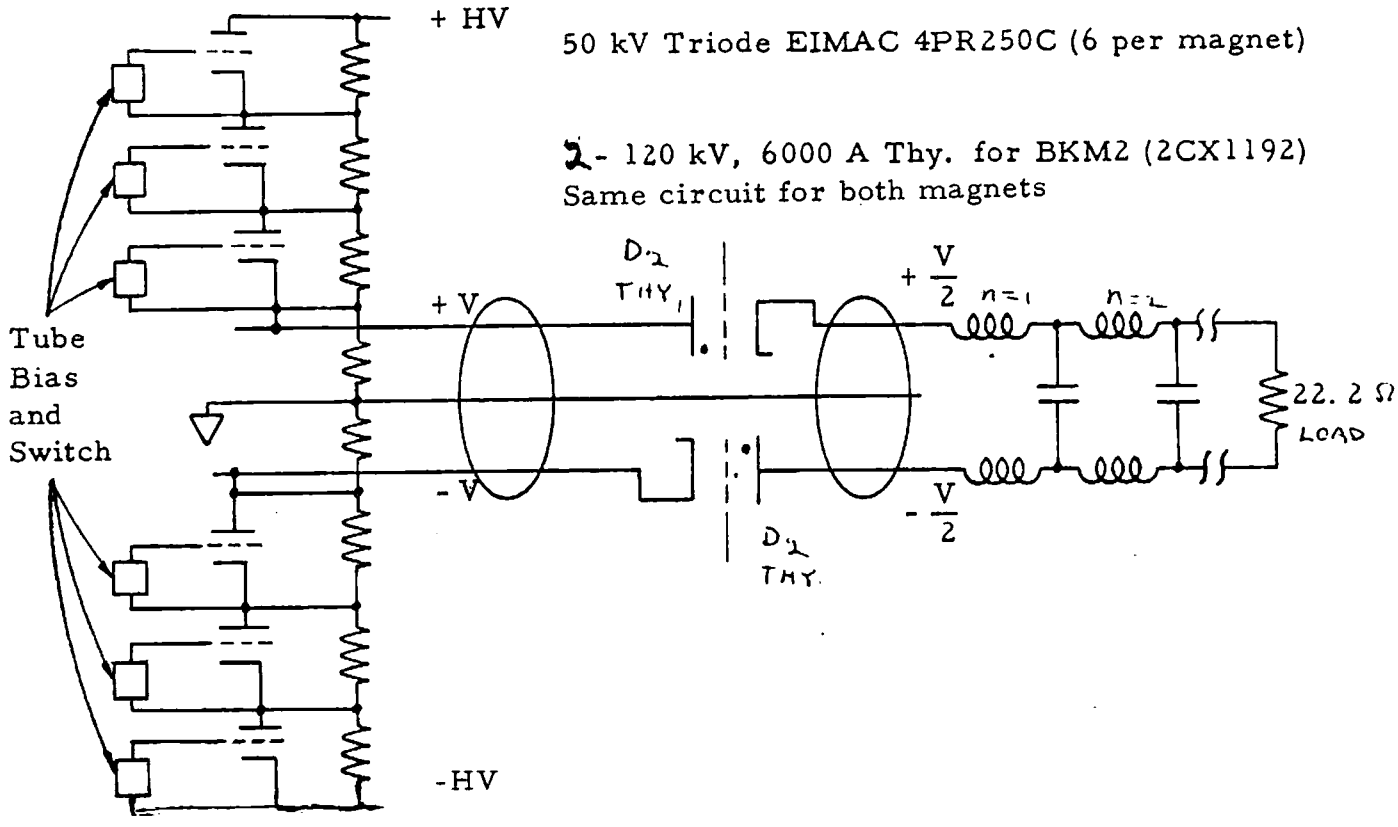

FIGURE 8 EXTRACTION KICKER CHARGING CIRCUIT

E. Vacuum System

The circumference of Booster II is very nearly 1/4 the circumference of the ZGS. The volume of its vacuum chamber basically consists of that volume between the polefaces and coils of 6 long magnets and 6 short magnets, plus that volume within 6 long straight sections and 6 short straight sections. Within this volume there is a surface area of approximately 400,000 cm^2. Expected outgassing of these surfaces will result in a continuous gas load of at least 7×10^{-4} torr-liters/sec.

Indium seals are used wherever possible so as not to raise the above gas load substantially. The metallic seals will also eliminate the certainty of downtime caused by radiation damage to elastomer type seals.

Pumping of the vacuum chamber is accomplished by one 500 liter/sec ion pump in each long straight section and one 400 liter/sec ion pump in each short straight section. The total effective pumping speed of these 12 pumps should enable the system to reach an average base pressure in the booster vacuum chamber of less than 5×10^{-7} torr.

The long magnets are valved at both ends because of their high impedance characteristics and the long term surface reconditioning required when they are subjected to atmospheric conditions. Besides eliminating the need of letting any long magnet up to atmosphere, these valves permit the letup to atmosphere of only one straight section without affecting the vacuum in the remaining volume of the booster

vacuum chamber. A straight section sector consists of one long straight section, one short straight section and one short magnet. The valves are pneumatically controlled and are interlocked to close when pressure in the chamber rises to some predetermined point.

Valves between the ion pumps and the straight section boxes are desirable but not absolutely essential. The ion pumps and the straight sections are equipped with heating sources or mantles to decontaminate surfaces rapidly during pumpdown.

Pumpdown to ion pump starting pressures is done with trapped 240 liter/sec turbomolecular pumps backed by properly sized rotary-piston or vane type roughing pumps. Two such pumping stations should be adequate since they are mobile for transfer from one sector to another.

Installation and removal of straight section boxes and/or ion pumps are done by a mobile vehicle such as a fork truck. This mobility is essential during assembly, disassembly, replacement, and routine maintenance to cut down time to a minimum.

F. RF Accelerating System

The accelerating rf potential is provided by two ferrite loaded coaxial cavities located in long straight sections L-2 and L-5. Each accelerating cavity contains 40 Ferroxcube 4H ferrite rings which allow the cavity to be tuned from 2.2 to 5.3 MHz. The current bias for the ferrite is provided by two figure-eight water-cooled copper windings. A bias current of 700 A at 5.3 MHz is required. This is provided by a 6 V, 1000 A, programable power supply. The cavity is 52.25 in. long, flange to flange, and contains a centrally located ceramic vacuum gap of 0.560 in. The gap is capable of operating at a voltage of nearly 12,000 V without breakdown or thermal runaway. Fig. 9 is a drawing of the accelerating cavity designed for Booster-II. An rf power of about 21 kW is required to develop the maximum peak voltage of 10,500 V per cavity.

Each cavity is provided with rf power from its own final power amplifier. The final rf amplifier has been designed to satisfy the peak average power demands of the cavity, the beam, and the additional power requirements of a set of traps which will be inserted (if needed) across the gap to control the harmonic-cavity induced voltage. With a set of traps to be described later, this will require a final amplifier with output capability of over 82 kW.

The final amplifier configuration is shown in Fig.10. It uses two 8752 triodes in a push-pull common-grid circuit. The amplifier is operated class A during the beginning and at the end of the acceleration

cycle to achieve lower output impedance. During the central portion where greater power is required it operates class AB. As a class AB amplifier it is capable of over 100 kW of output power when supplied from a 10 kV, 20 A power supply.

The traps which were mentioned previously are used to lower the gap impedance at the fundamental (5.3 MHz) and first harmonic frequency at extraction. They are necessary so that the gap voltage at extraction can be precisely controlled to keep the beam energy spread small. With large beam currents (4.2 A average at 500 MeV) and large gap impedance, small rf control voltage errors will cause large voltage changes across the gap. In addition, in order to keep harmonic induced voltages small, the gap impedances at the harmonic frequencies should also be small. The harmonic beam currents produce voltages across the gap proportional to the gap impedance shunted by the output impedence of amplifier.

The traps are two series resonant RCL circuits resonant near the fundamental and the first harmonic frequencies at extraction. The first circuit consists of a 50 Ω resistor, 15.6 μH inductor, and 47.6 pF capacitor, all in series, resonant at 5.84 MHz; the second, a 10 Ω resistor, 9 μH inductor, and 25 pF capacitor resonant at 10.61 MHz. The impedance of the gap with the above across it is $73\angle -75^{\circ}\ \Omega$ in polar form at 5.3 MHz. The impedance is low enough that a practical phase control of ± 3 degrees is required. The harmonic components

of the voltage across the gap in polar form are shown in Table IV at various times and frequencies. The table indicates that the harmonic component is small throughout the whole acceleration cycle and therefore may not be a problem.

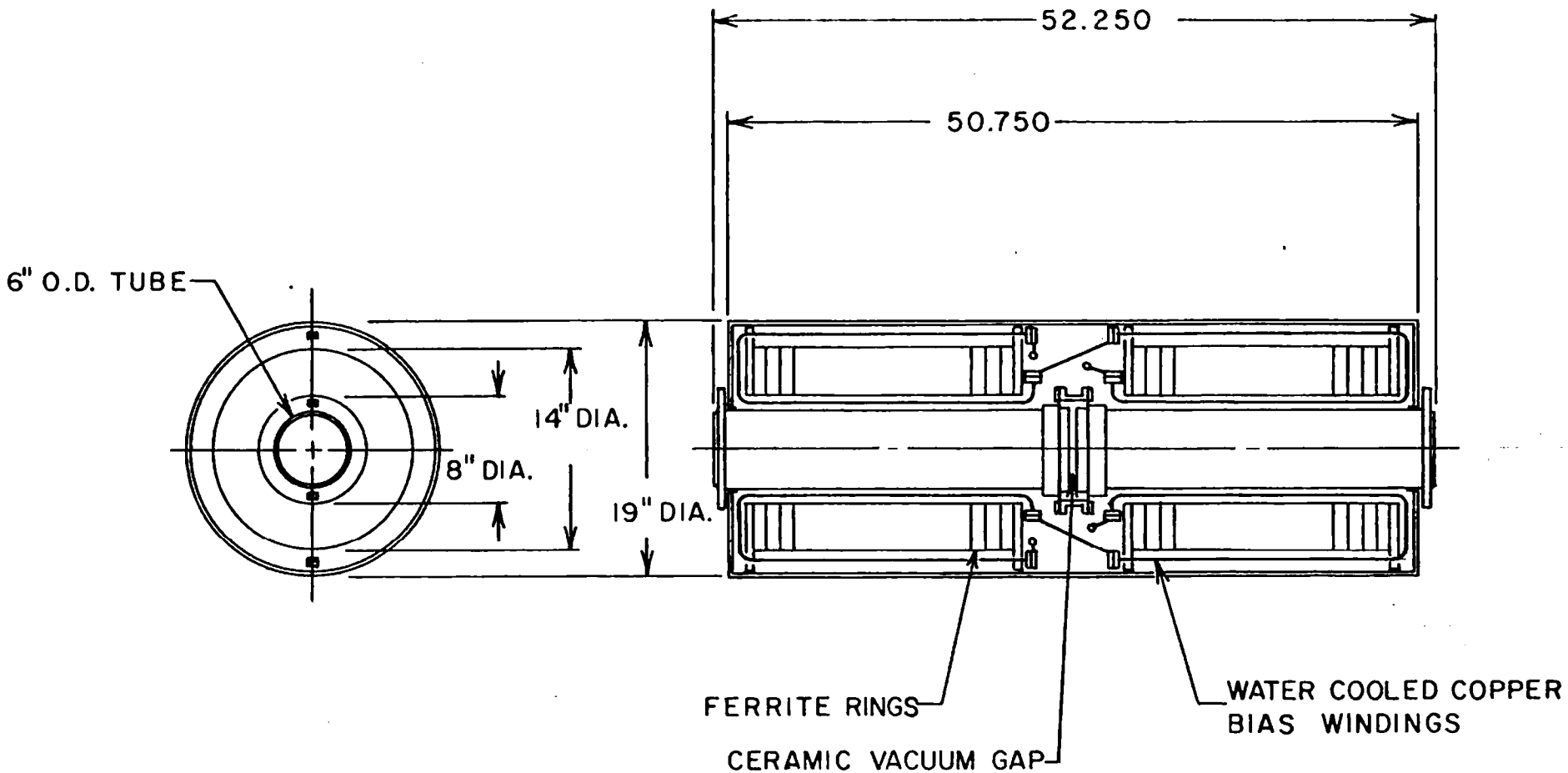

FIG. 9 BOOSTER II R.F. ACCELERATING CAVITY

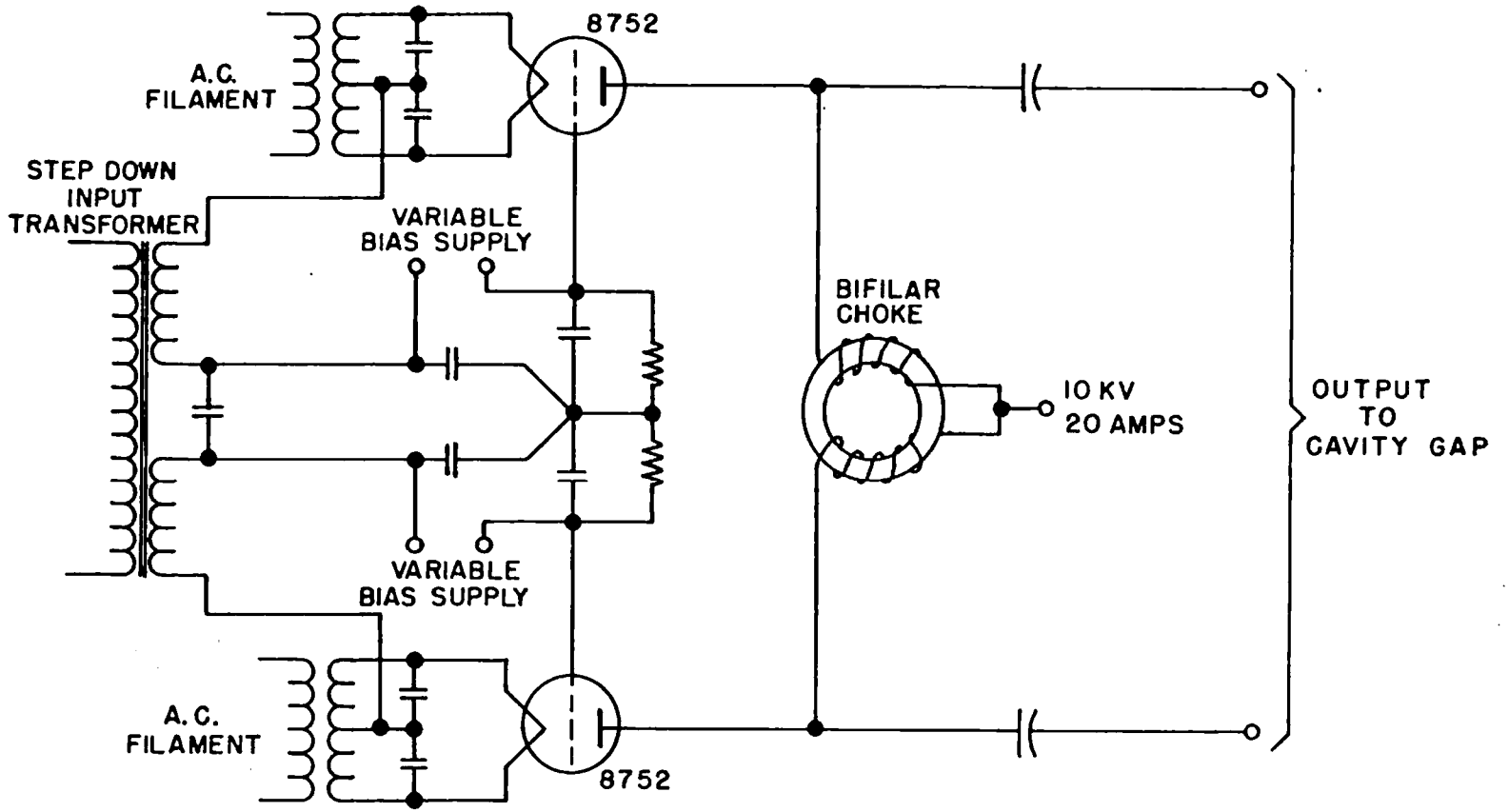

FIG. 10 BOOSTER II FINAL POWER AMPLIFIER

TABLE IV

HARMONIC COMPONENTS OF GAP VOLTAGE

IN POLAR FORM

Time msec	Fundamental frequency F in MHz	V1 at 1 x F in Volts	V2 at 2 x F in Volts	V3 at 3 x F in Volts	V4 at 4 x F in Volts	V5 at 5 x F in Volts
0.318	2.200	$512\angle -35^\circ$	$77\angle -238^\circ$	$152\angle 152^\circ$	$18\angle -260^\circ$	$38\angle -120^\circ$
4.570	3.000	$8087\angle -30^\circ$	$73\angle -100^\circ$	$33\angle 74^\circ$	$69\angle 101^\circ$	$15\angle -185^\circ$
7.074	3.800	$10219\angle -30^\circ$	$246\angle -100^\circ$	$26\angle -117^\circ$	$14\angle 70^\circ$	$9\angle 90^\circ$
16.400	5.290	$597\angle -80^\circ$	$18\angle -25^\circ$	$3\angle -70^\circ$	$17\angle -180^\circ$	$10\angle -180^\circ$
16.666	5.293	$50\angle -89^\circ$	$18\angle -25^\circ$	$3\angle -70^\circ$	$17\angle -180^\circ$	$10\angle -180^\circ$

G. Ring Magnet Power Supply (RMPS)

1. General

The booster ring magnets are excited with a 30 Hz, biased sine wave current. Series capacitors are used to form a resonant network with the magnets. This network is excited by a programmed solid-state power supply. It is necessary to provide a bypass for the dc-bias current around the capacitors. This bypass is accomplished by putting a choke in parallel with the capacitors and resonating the resulting tank circuit at 30 Hz. The betatron frequency of the synchrotron is 2.2. In order to minimize second harmonic perturbations, the ring magnets are powered from one feed point as illustrated by Fig. 11.

Neglecting saturation effects, the time-variation of the magnet current, i_M, is given by

$$i_M = I_{dc} - I_{ac} \sin \omega t \ ,$$

where I_{dc} is the bias current and I_{ac} is the 30 Hz current. The resonant frequency of the network is given by

$$\omega_o = \left(\frac{L_M + L_{CH}}{L_M \times L_{CH} \times C} \right)^{1/2} \ ,$$

where L_M is the inductance of the ring magnets, L_{CH} is the choke inductance and C is the capacitance of the resonant capacitor bank. The capacitor and choke currents are given by

$$i_C = - \frac{L_M + L_{CH}}{L_{CH}} I_{ac} \sin \omega t \ ,$$

$$i_{CH} = I_{dc} + \frac{L_M}{L_{CH}} I_{ac} \sin \omega t \quad .$$

The current wave forms of the magnet, capacitor and choke are shown in Fig.12 together with the voltage waves. The equivalent 30 Hz resonant circuit of the installation is shown in Fig.13.

2. Component Parts

a. Capacitors

A total capacitance of approximately 3000 μF is made up from capacitors rated at 9.5 μF, 3800 V rms, 60 Hz. They are assembled in three blocks, each block containing three rows of 38 capacitors. Of the total of 342 units mounted, approximately 316 are used. These capacitors were formerly used at CEA.

b. Choke

The ring magnets of BST-I (the former 2.2 GeV Cornell synchrotron) are used as bypass chokes. Twelve magnets are connected in series to obtain a choke inductance of 16 mH.

c. Power Supply

Phase-controlled solid-state power supplies drive the biased 30 Hz current through the series resonant circuit. The power supplies are connected to the 13.2 kV line through an isolation transformer. This keeps commutation noise, generated by the

phase-controlled power supplies, from interfering with equipment connected to the 460 V line that feeds all the other booster facilities. A 24-phase rectifier system is obtained by shifting, with an autotransformer, the 3-phase 460-V input voltages to the two identical 12-phase power supplies by 15° with respect to each other, and connecting the dc outputs in series. The predominant 24th-harmonic ripple current produced by the power supply is filtered by a low pass filter and by the series tuned LC circuit of the magnet load. Due to unbalance of impedance or ac line voltage, harmonics of order 1, 2, 3, etc., on the dc side and 2, 3, 4, on the ac side may appear. These harmonics are reduced by forward feeds from the line voltages to the rectifier phase control circuits.

In Fig. 12 the power supply current and voltage waves are shown. Since the power supply voltage has to be inverted, no free-wheeling diodes can be used for magnet protection. SCR's with overvoltage trigger circuits backed up by spark gaps are used for this purpose.

Table V lists the parameters of the booster power supply. The sum of the ac and dc losses is ~ 490 kW, the peak power is 1.35 MVA. Two 12-phase power supplies, each rated at 2.5 kA, 200 V (500 kW), and a 1.3 MVA autotransformer furnish this power as illustrated by Fig. 14. The interconnection between these power supplies is also connected to ground through a ground fault detector. This ground connection limits the peak voltage on the capacitor bank to $\pm$ 2.8 kV with respect to ground.

The power supply uses SCR-phase control to produce and regulate its output efficiently. A high gain amplifier compares a voltage proportional to the magnet current with a precision reference voltage and controls the SCR firing circuits in a closed loop circuit. A current transductor is used to monitor the magnet current. Its output is 10 V for a 5 kA input. The reference signal is composed of a variable 30 Hz voltage biased by a variable dc voltage.

d. Interconnections

Dipole fields, excited in the straight sections by the current in the interconnecting buswork, should not exceed 0.1% of the field in the magnets. Therefore, during injection these fields must be $\leq$ 2.8 G. It is customary to eliminate practically stray fields by arranging the buswork in a foldback arrangement as shown in Fig. 15 a However, such an arrangement requires twice as much copper, support structure, and space, and much more labor to install than single loop connections illustrated by Fig. 15b. A single loop installation suffices by separating the interconnecting cables from the beam orbit by $\geq$ 75 cm. The interconnections are made with six 500 MCM, 5 kV cables connected in parallel.

e. Protection

1) The power supplies are protected against:

ground fault

over current

SCR failure

control power failure

insufficient cooling

In addition there are door interlocks to prevent access to energized equipment.

2) Magnets and chokes are monitored and protected against:

loss of water

ground faults

over voltage

voltage unbalance

temperature unbalance

3) Each capacitor in the 3000 μF bank is fused.

Table V

Parameters of Booster Power Supply

Ring Magnets	dc current	2300 A
	ac rms current	919 A
	total rms current	2477 A
	total magnet voltage	5590 V
	peak magnet voltage to ground	2795 V
	inductance of all magnets	22.8 mH
	maximum stored energy	147.7 kJ
	ac losses	68.6 kW
	dc losses	230.6 kW
Choke	dc current	2300 A
	ac rms current	1310 A
	total rms current	2647 A
	inductance of choke	16.0 mH
	maximum stored energy	137.9 kJ
	ac losses	61.8 kW
	dc losses	84.6 kW
Capacitor	ac rms current	2229 A
	maximum stored energy	46.8 kJ
	ac losses	26.4 kW
Cable losses		15 kW
Total losses		487 kW

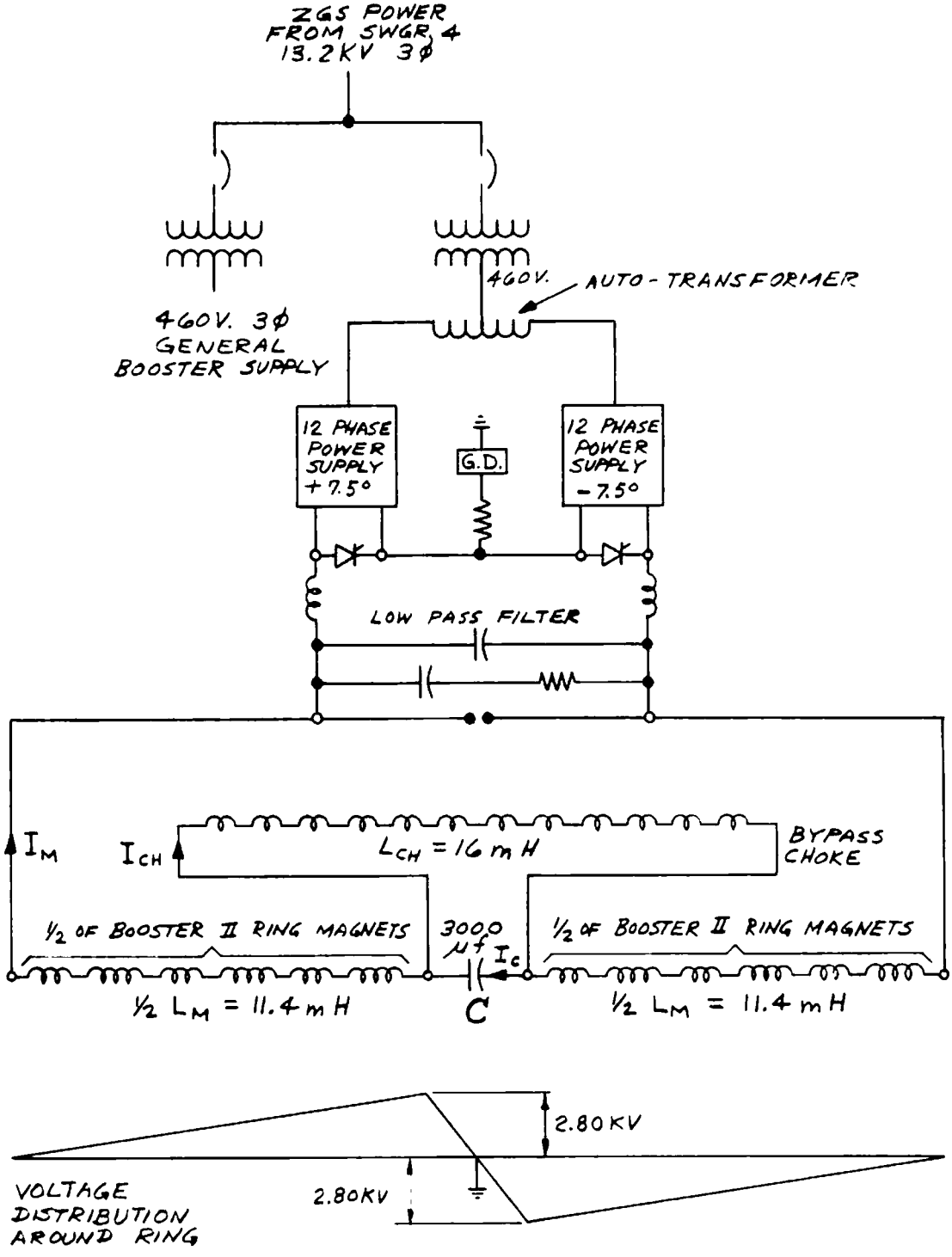

FIG. 11 BOOSTER II RMPS

FIG. 12 WAVEFORMS OF RMPS VS TIME

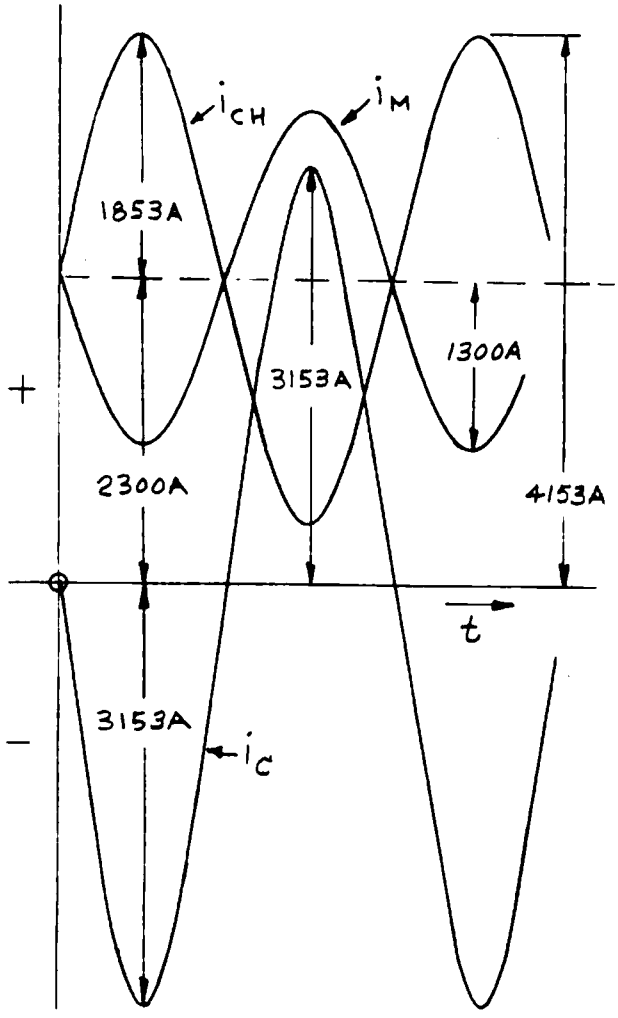

MAGNET (i_M), CHOKE (i_{CH}) AND CAPACITOR CURRENT (i_C)

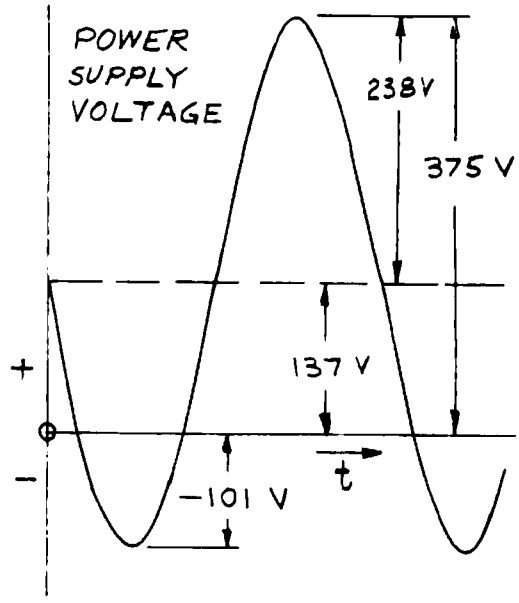

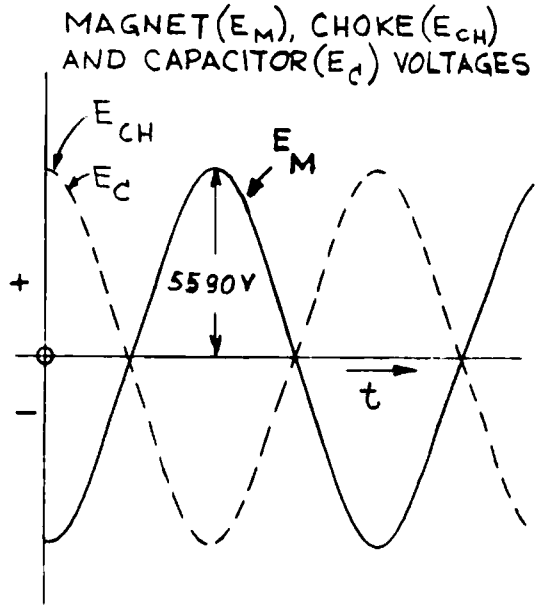

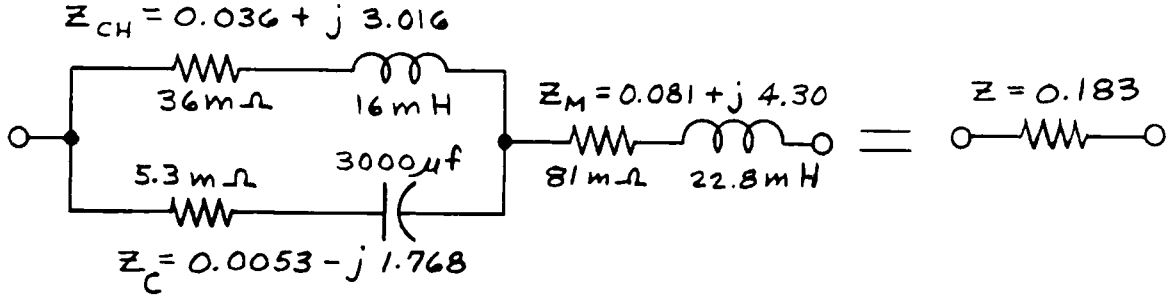

FIG. 13 EQUIVALENT RESONANT CIRCUIT OF RMPS

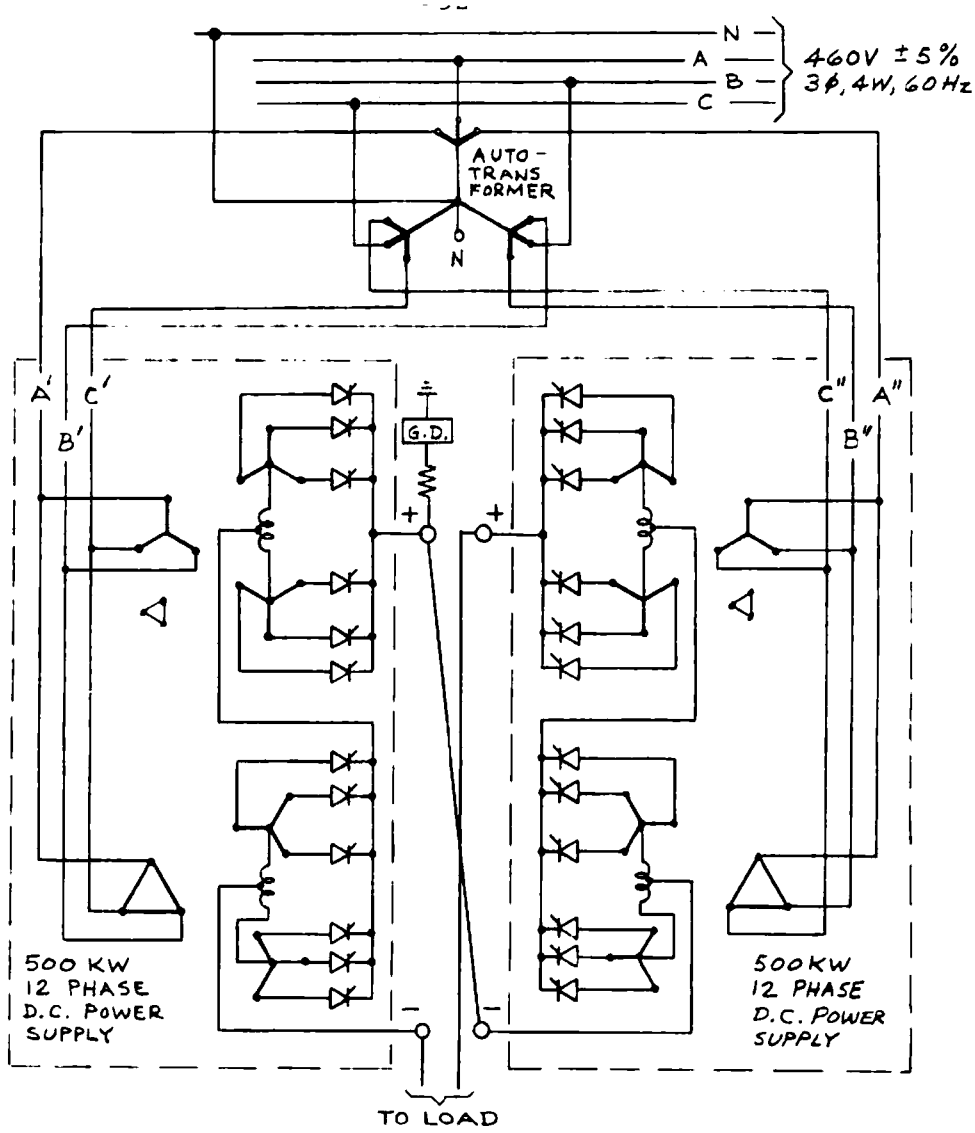

FIG. 14 24 PHASE DC POWER SUPPLY COMPRISING AN AUTOTRANSFORMER PROVIDING ± 7.5° PHASE SHIFT AND TWO IDENTICAL 12 PHASE DC POWER SUPPLIES CONNECTED IN SERIES.

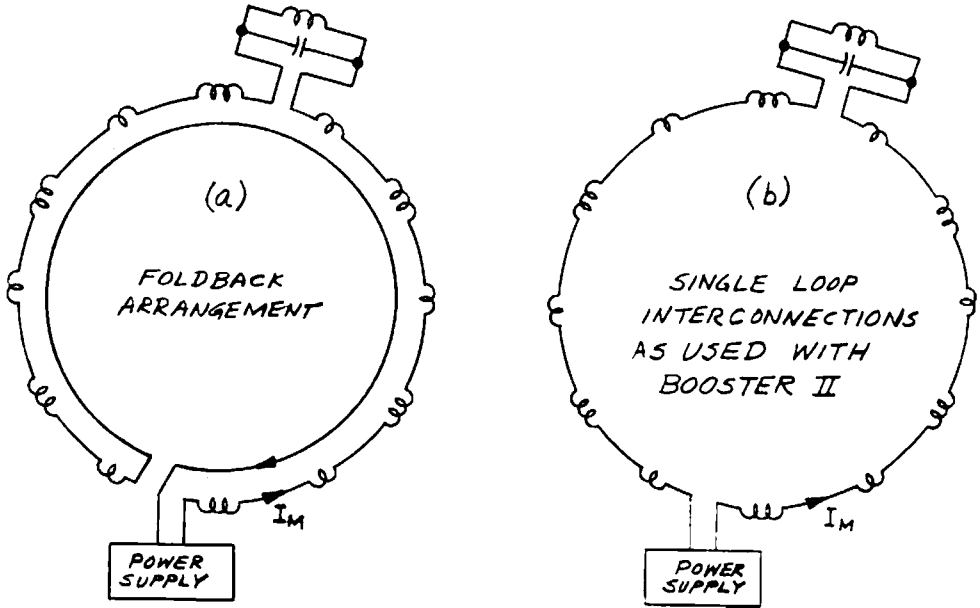

FIG. 15
INTERCONNECTING BUSWORK FOR RING MAGNETS

Section III

Intensity Related Effects

A. Space Charge Limit

The space charge forces between a particle and the beam modify the effective focusing force and make the betatron frequencies intensity dependent. The beam intensity must be less than a value that would shift the betatron frequency to the nearest linear or quadratic resonance. In the booster, as in most other accelerators, the vertical dimension of the beam smaller than the horizontal dimension and the space charge limit is primarily determined by the allowable vertical betatron frequency shift. For a beam of elliptical cross section with horizontal semi-axis, a, and vertical semi-axis, b, the space charge limit is given by

$$N = \frac{\pi \nu_v \Delta \nu_v b(a+b) \beta^2 \gamma^3 BF}{r_p R}$$

where ν_v is the vertical betatron frequency; $\Delta \nu_v$ is the allowable shift in ν_v, r_p is the classical proton radius ($\approx 1.54 \times 10^{-18}$ m), R is the mean radius of the booster and B is the bunching factor, approximately given by

$$B = \frac{\text{(bucket phase area)}}{2\pi \text{ (bucket height)}}$$

During capture in a stationary bucket, $B \leq 2/\pi$ but reduces very quickly to less than 0.5 as soon as $\dot{B} \neq 0$.

The quantity F is a factor determined by the image current and charges. It is given by

$$F = \frac{1}{1 + \frac{b(a+b)}{n^2}\left[\varepsilon_1 (1+B\gamma^2\beta^2) + \varepsilon_2 B\gamma^2\beta^2\left(\frac{h}{g}\right)^2\right]}$$

where h is the half height of the vacuum chamber and g is the magnet half gap. For a rectangular vacuum chamber with half width $w >> h$ and $h >> \sqrt{a^2 - b^2}$ the image coefficients are given by $\varepsilon_1 = \pi^2/24$. In the booster, with a = 0.95 in., b = 0.7 in., h = g = 1.25 in., γ = 1.0576, β = 0.39, and B = 0.45, this yields F = 0.85. The beam envelope varies in dimension along the circumference of the booster as

$$b = \sqrt{\beta_v Q_v}$$

and

$$a = \sqrt{\beta_h Q_h}$$

where β_v and β_h are respectively the vertical and horizontal beta-functions and Q_v and Q_h are the vertical and horizontal beam qualities.

In the booster

$$\left\langle \frac{\nu_v \beta_v}{R} \right\rangle \approx \langle \sqrt{\beta_v \beta_h} \rangle \approx 1.15$$

and the expression for the space charge limit becomes

$$N \approx 3 \frac{Q_v + \sqrt{Q_v Q_h}}{r_p} \Delta\nu_v \beta^2 \gamma^3 B$$

Substitutions of $Q_v = 3.8$ [mrad - in.] $= 10^{-4}$ [rad - m], $Q_h = 7.$ [mrad - in.] $= 1.78 \times 10^{-6}$ [rad - m], $\Delta\nu_v = 0.25$, $\gamma = 1.0556$, $\beta = 0.32$, and $B = 0.45$, leads to

$$N \approx 5.6 \times 10^{12}.$$

In this calculation it is assumed that the particle distribution within the bucket is uniform. The actual space charge limit could be slightly smaller due to nonuniformity in the distribution.

B. Collective Instabilities

1. Unbunched beam longitudinal instability

The beam in the booster is unbunched during injection. The booster operates below the transition energy, so longitudinal instability could occur only for a resistive and/or inductive wall. In general, the vacuum chamber walls are capacitive and slightly resistive. An effectively inductive wall could occur in the rf cavities. The stability condition is given by the relation

$$I Z_{11} < \eta \gamma U_o \left(\frac{\Delta E}{E}\right)^2$$

where I = Nef = circulating beam current

Z_{11} = coupling impedance (resistive and/or inductive)

$$\eta = \frac{1}{\gamma_t^2} - \frac{1}{\gamma^2} \; ; \gamma_t = \text{transistion energy}$$

$$U_0 = \frac{mC^2}{e} \approx 9.38 \times 10^8 \text{ V}$$

In the booster, the vacuum chamber walls are formed by the pole tips. The resistive coupling impedance is approximately given by

$$Z_{11} = \frac{\pi R}{b} (1 + i) R_s$$

where R is the booster radius, $R_s = \sqrt{\frac{W_o \mu \mu_o \rho}{2}}$ is the surface resistance, b is the width of the pole tip, ρ and μ are respectively the resistivity and the permeability of the wall material, and W_o is the angular velocity of the particle. The effect of the insulation between the laminations is neglected. Matching the invariant bucket area of the booster with that of the ZGS with V = 24kV and B = 17 kG/sec, we find the stability limit.

$$\text{At injection } Z_{11} < 70 \text{ ohm}$$

$$\text{At 500 MeV } Z_{11} < 90 \text{ ohm}$$

In the booster, R = 6.84 m, b ≈ 0.16 m, $W = 2\pi \times 2.2 \times 10^6$ at injection, and $W = 2\pi \times 5.3 \times 10^6$ at 500 MeV. Assuming μ = 400 and

$\rho = 5 \times 10^{-7}$ ohm-m for the lamination we find

$$|Z_{11}| \approx 8 \text{ ohm at injection}$$

and

$$|Z_{11}| \approx 9 \text{ ohm at 500 MeV} .$$

These coupling impedances are considerably lower than the stability limit. The coupling impedance of the rf cavity is more difficult to estimate. However, because the injection time is less than 500 μsec and the growth rate of the spontaneous bunching is of the order of milliseconds or longer, it is not likely that spontaneous bunching will occur during the injection.

Similar calculations for transverse instability indicate that such instabilities will not be troublesome for unbunched beam.

2. Bunched beam longitudinal instability

There is only one bunch in the booster and the simplest coherent mode is the rigid dipole bunch motion. For a smooth circular vacuum chamber the growth rate of the resistive wall instability is given by (2)

$$\frac{1}{2} = 0.0134\, \Omega_s \, \frac{|Z_{11}|}{V \cos \varphi_S} \, I\, G\, (\nu_s)$$

where $\Omega_s = \frac{W_o}{\beta}\sqrt{\frac{|\eta| e V \cos\varphi_s}{2\pi E_s}}$ is the synchrotron frequency. $\nu_S = \frac{\Omega_S}{W_o}$ is the synchrotron frequency per turn, and $G(\nu_S) = \sum_{k=1}^{\infty} \frac{\sin 2\pi k\nu_S}{k}$. In the booster at injection, $|\eta| = 0.65$, $V\cos\varphi_s = 1.88$ kV, $I = 1$ A, $\beta = 0.314$, $E_s = 988$ MeV, and $|Z_{11}| = 8$ ohm. Noting that $G(\nu_s) < 1$, we find $\frac{1}{\tau} < 2$ or $\tau > 500$ msec, very much longer than the accelerating period.

The vacuum chamber is not circular, but the value of τ is so large that it is very unlikely that bunched beam longitudinal instability will occur.

3. Bunched beam transverse instabilities

There are two classes of transverse instabilities to be considered: the rigid bunch instability and the head-tail instability. Consider first the rigid bunch type.

The choice of $k < \nu < k + \frac{1}{2}$ insures stability against resistive wall effects. However, dipole coherent instability is still possible due to the ions in the residual gas. Molecules of the residual gas will be ionized by the proton beam. For a bunched beam, the electrons, with their higher velocity, escape to the chamber walls in a time interval short compared to the rotation period of the beam. The velocity of the positive ions is unfortunately much smaller. The field of the ion cloud could cause instability. The equation of motion of a particular proton, neglecting incoherent space charge effect, is given by

$$M_o \gamma \left(\frac{d^2 Z}{dZ^2} + \nu^2 W_o^2 Z \right) = e \left[U_1 \bar{Z} + V_1 (Z - \bar{Z}_i) \right]$$

where $U_1 \bar{Z}$ is the transverse field generated by the coherent motion of the beam, $V_1 (Z , Z_i) = \frac{N_i e}{2\pi e_o a^2}$ is the transverse field due to the ion cloud, N_i is the number of ions per unit length, a is the radius of the cloud, and ξ_i is determined by the location of the proton beam at an earlier time. The ion cloud spreads in both transverse directions. We also assume that only the ion cloud of a previous turn remains in the vacuum chamber. Assuming harmonic oscillations of the proton beam center,

$$\bar{Z} = \xi_e \, i(wt-no),$$

and for a short single bunch we find

$$\bar{Z}_i = \bar{Z} \, (t - T) = (\cos \varphi - i \sin \varphi) \, \bar{Z}$$

where

$$\varphi = WT; \; T = \text{rotation period.}$$

Now $W = (n-\nu) W_o$, thus $\varphi = (n-\nu) 2\pi$. In practice we can neglect V_1 compared to $M_o \gamma \nu^2 W_o^2$. Replacing $\left(\frac{d}{dt} \right)$ by $\left(\frac{\partial}{\partial t} + W_o \frac{\partial}{\partial \theta} \right)$ we

obtain

$$M_o \gamma \left[\left(\frac{\partial}{\partial t} + W_o \frac{\partial}{\partial \theta} \right)^2 + \gamma^2 W_o^2 \right] Z = e(U + iV)\bar{Z}$$

where

$$U = U_1 - V_1 \cos\varphi \text{ and } V = V_1 \sin\varphi = \frac{N_1 e}{2\pi \epsilon_o a^2} \sin\varphi$$

Solving for Z gives,

$$Z = \frac{e(U + iV)}{M_o \gamma \left[\nu^2 W_o^2 - (w - n W_o)^2 \right]} \bar{Z}.$$

In the absence of frequency spread we obtain the relation

$$1 = \frac{e(U + iV)}{M_o \gamma \left[\nu^2 W_o^2 - (W - n W_o)^2 \right]}.$$

which can be rewritten in the form

$$W - (n - \nu) W_o = \frac{e(U + iV)}{M_o \gamma \left[\nu W_o + n W_o - W \right]} \approx \frac{e(U + iV)}{2 M_o \gamma \nu W_o},$$

since

$$W \approx (n - \nu) W_o .$$

The motion is unstable when the imaginary part of W is negative, i. e. when $V < 0$. This condition is satisfied when

$$n < \nu < n + 1/2$$

or

$$\sin \varphi = 2\pi (n-\nu) < 0 .$$

The growth rate is given by

$$\frac{1}{\tau} = \frac{eV}{2M_o \gamma \nu W_o} = \frac{N_i c^2 r_p |\sin \varphi|}{\gamma a^2 \nu_o W_o} ,$$

where $r_p = \dfrac{e^2}{4\pi \epsilon_o M_o c^2}$ is the classical proton radius ;

and

$$N_i = \frac{N \frac{dE}{dx} \frac{P}{760} P}{e V_i} \left[cm^{-1}\right] = \frac{100N \frac{dE}{dx} \frac{P}{760} P}{\left[m^{-1}\right]}$$

where N is the number of protons in the bunch, $\dfrac{dE}{dx}$ is the ionization loss in MeV/g/cm^2, ρ is the density of the residual gas, P is the pressure in torr, and eV_i is the required energy to produce one ion

pair. Assuming the residual gas is air and neglecting the ionization by primary and secondary electrons ($eV_i \approx 200$ eV) we obtain $N_i = 8.6\ pN\ M^{-1}$. Substitution of this in the expression for τ gives

$$\frac{1}{\tau} = \frac{8.6\ P\ N\ r_p\ c^2}{a^2\ \gamma\ \nu\ W_o} .$$

In the booster: $p = 5 \times 10^{-7}$, $N = 3 \times 10^{12}$, $a = 0,\ 0.03$ m, $\gamma = 1.0533$, $\nu = 2.32$, $W_o = 2\pi \times 2.2 \times 10^6$.

Thus

$$\frac{1}{\tau} = 59\ \tau = 17 \text{ msec for } N = 3 \times 10^{12}$$

or

$$\tau = 50 \text{ msec for } N = 1 \times 10^{12} .$$

The presence of frequency spread will decrease this growth rate so the rigid bunch instability will not be serious. Now consider "head-tail" instability.

The betatron frequency ν and the angular velocity W_o depend on the momentum of the particle. Therefore the betatron phase difference between a nonsynchronous particle and a synchronous particle varies as the particle moves from the head of the bunch to the tail (or vice

versa). The amount of this phase shift is given by

$$\chi = \frac{1}{2} \Delta (\nu W_o t_s) ,$$

where t_s is the synchrotron oscillation period. The rotation frequency W_o averaged over the period t_s is the same for all particles. That is ,

$$\Delta (W_o t_s) = \Delta W_o t_s + W_o \Delta t_s = 0.$$

Thus

$$\chi = \frac{1}{2} \Delta \nu W_o t_s = \frac{1}{2} \xi \nu \frac{\Delta p}{p} W_o t_s = - \frac{1}{2} \frac{\xi}{\eta} \nu \Delta W_o t_s$$

$$= \frac{\xi}{\eta} \nu W_o t_1 ,$$

where

$$\xi = \frac{p}{\nu} \frac{d\nu}{dp} ; \text{ the chromaticity ,}$$

and

$$\eta = \frac{1}{\gamma_t^2} - \frac{1}{\gamma^2} .$$

$t_l = \frac{l}{2} - t_s$ is the bunch length in seconds.

It can be shown that for small values of χ we have

$$\frac{1}{\tau} = K_{\chi} \quad ,$$

where the constant is positive or negative depending on the mode number. However, if the chromaticity $\xi = 0$, $\chi = 0$, then the growth rate τ is infinite regardless of the mode number.

4. Summary of Stability Considerations

Summarizing these stability considerations we have:

a. Instabilities during injection, while the beam is unbunched, are not expected to be a problem. Should bunching via coupling to the rf cavities occur, it will not be destructive.

b. Longitudinal bunched beam instabilities are expected to grow very slowly compared to the acceleration period and hence cause no trouble.

c. Transverse instability due to ionization of residual gas within the machine may require tune spread by octupole terms in the lattice. Such higher order corrections are planned for the machine. In addition, these calculations have assumed a mean pressure of 5×10^{-7} torr, whereas calculations made concerning the vacuum system predict perhaps half this value.

d. Head-tail instability must be eliminated by reducing the chromaticity of the machine to a small value. The sextupole magnets required for this are provided in the machine design.

REFERENCES

1. E. Keil, "Intersection Storage Ring," CERN 72-14, (1972).

2. F. J. Sacherer, Proceedings of the 1973 Particle Accelerator Conference, IEEE Trans. Nucl. Sci. NS-20, p-826.

3. F. J. Sacherer, "Transverse Bunch Beam Instability." Proceedings of the 9th International Conference on High Energy Particle Accelerators, 1974.

IV. BST/ZGS Beam Transfer

The 500 MeV beam from the booster is synchronously injected into nonaccelerating buckets in the ZGS with two booster pulses injected into each of the four ZGS buckets. The 4th harmonic is used, since the booster radius is one-fourth of the ZGS radius and the booster must operate on the first harmonic in order to meet the energy spread requirements of the ZGS and have sufficient time to energize the extraction and injection kicker magnets. The beam enters the ZGS in the outside upstream end of the L-1 straight section by means of the "40° magnet" which injects the beam at about 3° to the ZGS center line. The proper launch conditions are provided by a 33-in. long inflector magnet located in the downstream end of the L-1 straight section. The injector scheme is shown in Fig. 16. The kicker magnet is located in the S-2 straight section, which is 112° away from L-1 in betatron space, assuming a radial tune of 0.833. The first booster pulse is kicked onto the equilibrium orbit and allowed to circulate there until the next booster pulse is ready. Three turns before the next pulse is injected, the beam is kicked a second time so as to produce an oscillation amplitude which will just miss the inflector magnet. After three turns, this bunch is back at the S-2 kicker along with the next booster pulse and together they are kicked so as to center the CG of these two bunches around the equilibrium orbit. This process is then repeated for the next ZGS bucket until all four are filled.

The diagrams of Fig.16 assume the beam has the same momentum dispersion at the inflector as it has in the ZGS. This produces the

minimum beam size in the ZGS. This degree of dispersion cannot be exactly produced by the 500 MeV beam line, so the actual beam size will be slightly larger. If the beam has no dispersion, i. e., it is recombined at the inflector, the beam size is $\frac{3R}{\nu x} \frac{\Delta p}{p}$ in. larger than minimum. This corresponds to ~1. 8 in. for the design energy spread of ±400 keV.

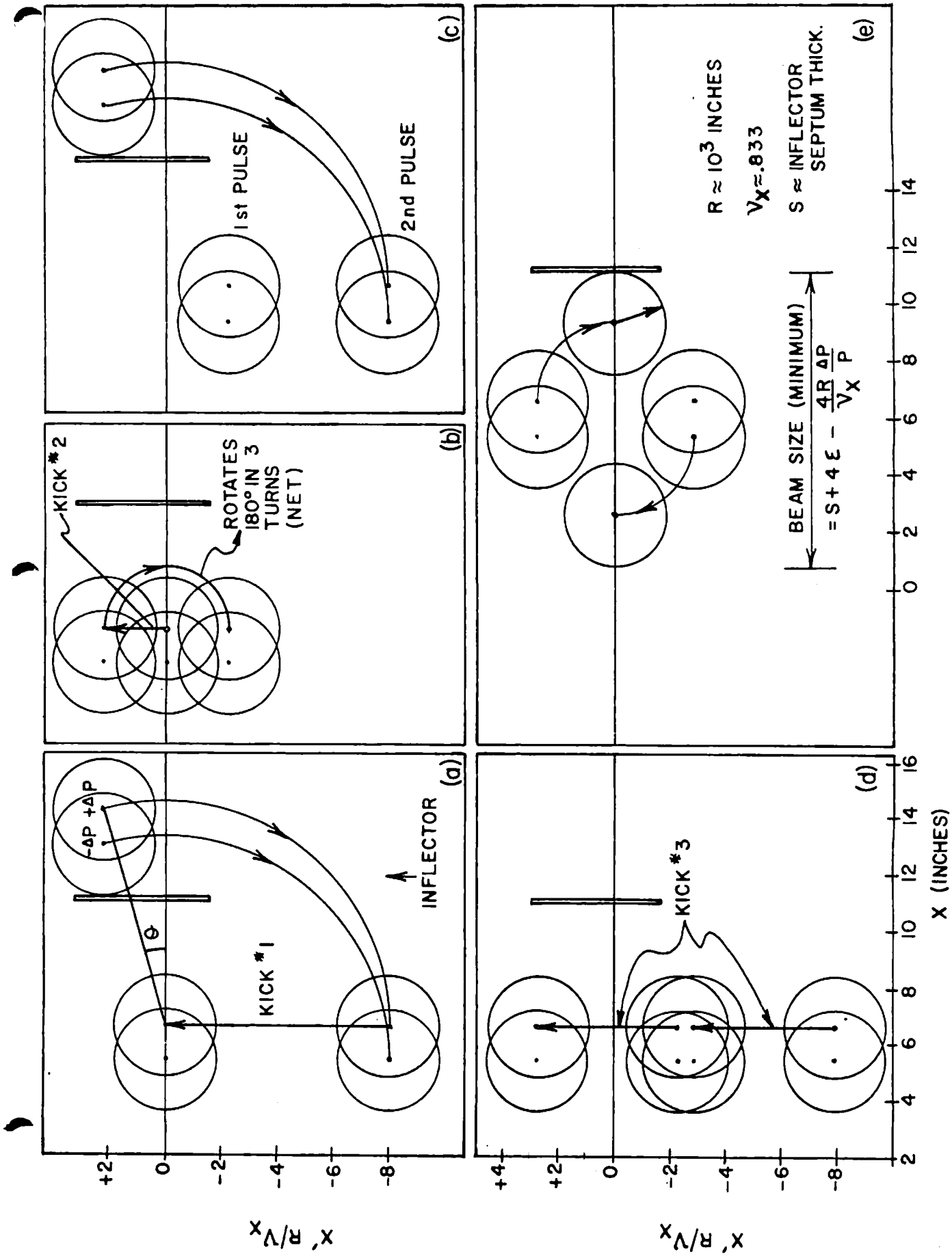

FIG. 16 ZGS INJECTION SEQUENCE

V. Beam Line Modifications

A. 50 MeV Transport

BST-II injection will be into the BST-I straight section, through the D1 magnet to a stationary stripper located in BL1. Beam calculations, tracing matched parameters backward through TRIM calculated fields indicate that a horizontal waist is required at the match point. The vertical requirement is for a beam that is slightly converging as it goes toward the booster.

It is necessary to modify the transport because synchrotron matching between the booster and the ZGS requires an energy spread into the booster of ±100 keV or less. Since this is about a factor of three less than that of the linac beam, it is necessary to provide a debuncher in the linac-to-booster transport. This will be accomplished by moving the existing debuncher (in the linac to ZGS line) to a location between the magnet shelter and the booster building.

The debuncher aperture is 2 in. This requires adjusting the beam elements to produce a waist in both the horizontal and vertical planes at the debuncher location. Calculations with MAYPO[1] show that this can be achieved with the existing elements.

The beam line between the debuncher and the BST-II injection point will be modified to contain two pairs of quadrupoles to permit matching the beam from the debuncher into BST-II. Two of the three bending magnets will be used to provide a nonachromatic bend just upstream of the BST-II. A fifth vertically focusing quadrupole

is required between the bending magnets and BST-II to permit matching the vertical phase space without interference from the vertical aperture limits of the bending magnets. MAYPO calculations indicate that a good match can be obtained with this system.

Tuning of the debuncher will be done with the aid of a slit located downstream of the debuncher and with a beam width detector located at the match point. The nonachromatic bend between functions as a momentum spectrometer.

A few additional beam width sensing devices will be installed at critical points to make it possible to properly adjust the two achromatic bends in the line between the linac and the debuncher.

---

[1] G. Concaildi, R. George, and S. Marcowitz, "MAYPO, an On-Line, Real-Time Beam Optics Program," ARF Internal Report GAC/RDG/SMM-3 (October 20, 1971).

B. 500 MeV Beam Line

The 500 MeV beam line takes the beam from the extraction septum magnet and transports it to the ZGS with the proper phase space orientation and dispersion. The line consists of eight quadrupoles and four bending magnets. The beam is bent from the extraction chain into the booster-ZGS transfer tunnel in two separate 15^{o} bends using 10-IV-36 magnets opened up to 6-in. gaps. They are powered in series by a single Transrex PS already located in that area. The bend into the ZGS is likewise a two-step process using a 24-VIII-36 and a 40^{o} wedge mounted in the L-1 straight section box cover. These two magnets are likewise powered by Transrex PS to be located at the end of the linac building where adequate primary power exists. The quadrupoles are powered by the same PS installed for 200 MeV operations.

VI. Instrumentation

A. Control

Almost all control functions required by BST-II are counterparts of BST-I. Most of the existing main control room equipment will, in fact, be used with BST-II. The concept of having all normal operation controls in the main control room will be continued.

B. Diagnostics

1. Transports

Diagnostic systems provide information concerning beam current, position, and profile as an aid in beam line tuning.

The 50 MeV line currently has ion collection profile monitors (PAPS), beam toroid transformers, and Faraday cups. These devices will remain. The 500 MeV transport is equipped with fast toroid transformers at each end with which the extracted pulse shape and amplitude may be monitored. Beam profile monitors have been designed and tested which use secondary emission from very thin (7000 Å) aluminum strips. This permits "nondestructive" monitoring of the beam during normal use.

Sufficient instrumentation will be provided to deduce the emittance of the extracted beam. Whether this will be from the profile monitors or a slit arrangement has not yet been decided.

2. Synchrotron

The availability of adequate diagnostic systems for the synchrotron is extremely important for efficient start-up and operation. Diagnostics planned for the synchrotron include:

a. Beam transformer - to monitor the average circulating current in the machine.

b. Horizontal and vertical position monitors - placed in at least every period, they provide important information about orbit imperfections and facilitate corrections. They are also used as coherent motion monitors. It has not yet been determined if these devices will be of electrostatic or electromagnetic induction types, both of which would be applicable.

c. Beam profile - A beam profile for each transverse plane is provided in a location near a respective large-β point in the lattice. These will be of ion-collection design.

d. Aperture probes - Consideration is being given the possibility of having rapidly plunging, movable probes. These would facilitate accurate measurements of beam size and position.

e. Induction probes - These provide signals for use with bunch analysis, fast "Q", and phase feedback to the rf system.

f. Tune measuring equipment - coherent beam "wobbles" will be induced by the application of small electrostatic

excitation fields produced between parallel plate electrodes. Tunes can then be calculated from characteristics of beam response.

g. Radiation Monitors - not only will ionization-type loss monitors be useful for extraction system adjusting, but information about the location of losses will be helpful for orbit corrections.

VII. Booster II Installation

A. Procedure

With the completion of the tests with Booster I and before the installation of Booster II, it is necessary to remove the shielding presently used for Booster I. This shielding will be stored until such time as it is to be reinstalled over Booster II. This will probably be for a period of six or eight months.

Before the shielding can be removed, it is necessary to remove the services and equipment which are presently attached to the shielding. This requires several man weeks of effort by both ANL personnel and contractors.

After the removal of the shielding and Booster I from the building, the test borings for the new foundation will start followed as soon as possible by the installation of the foundations.

While the foundations are being installed, the present magnets of Booster I will be modified as necessary, and made ready to be reinstalled as the choke for the Booster II power supply. The choke also requires the two spare magnets be taken from the storage and installed with the other BST-I magnets at this time. The present magnet support beams will be machined at this time for the necessary modifications for use as supports for the new magnets. Both of the above operations will require a large work and storage area with overhead crane. At the time of the installation of the foundations, a

system of permanent bench marks and survey points will be installed for magnet alignment.

Due to the lack of an overhead crane in the actual booster building, it will be necessary to install the shielding side walls, ring magnets, rf cavity, heavy power supplies and choke in the center of the ring at the same time. After the installation of the roof shielding, the services can be reinstalled around the ring.

After services are completed, installation of straight section components and vacuum plumbing will be done in conjunction with main ring magnet installation.

B. Ring Foundation

The foundations for the Booster II magnet will be isolated from the adjacent floor on which the shielding and other equipment rest. Experience with Booster I has shown that when all equipment is on the existing common floor, it is impossible to maintain the required ±0.002 in. vertical stability of the booster magnet sections.

In Booster II, there are six long magnet sections, each weighing about seven tons and six short magnet sections, each weighing about two tons. Each long magnet section will be supported by two reinforced concrete posts and each short magnet section by one concrete post. All concrete posts will be identical. Each post will be 24 in. diameter and will be poured directly into a "post hole" with any subgrade

forms. The poured concrete will be supported and formed above grade by a thin wall, 20 in. diameter steel pipe, this being a warehoused, stock item.

It is expected that the ground bearing load is about 3000 lbs/ft^2. Test bores shall be made to substantiate this value.
Each post can therefore be loaded to about 9400 lbs which compares to about 7500 lbs and 8000 lbs expected load on the long and short magnet sections respectively.

Any equipment that is located in the straight sections and which requires precise alignment with the magnet sections will be supported by structural steel beams which will span between concrete posts. In this manner all magnets and straight section equipment will be isolated from the surrounding floor on which concrete shield blocks are located.

The structural steel supports presently used on the long magnet sections of Booster I shall be modified and reused for Booster II. New structural supports will be furnished for the short magnet sections.

Additionally, there will be six posts used for alignment purposes. These will be appropriately placed to form a hexagon and they will be independent of both the adjoining floor and the magnet support system.

C. Alignment Procedures

In designing an alignment system for Booster II, an external hexagonal control system was decided upon. It consists of six

steel circular monument posts, on which adjustable instrument mounting heads will be installed.

The magnets when constructed will have precision busings located on each end and side at the median plane, so that standard optical tooling procedures can be used to position the magnets once the monument system is established. Positional requirements have been established as vertical position (level)± 0.002 [in.], radial position ± 0.020 [in.], and axial position ± 0.020 [in.]. Equipment to be used in alignment include theodolites, transits, optical levels, stick-mikes, tapes, and tooling scales.

In addition to the optical alignment to be provided, a commonly connected hydraulic reference system will be installed to provide rapid readout of changes in magnet level within 0.002 in. The basic system consists of a centrally located reference vessel connected in series with similar vessels attached to each end of all booster ring magnets. Electronic readout for changes in level are being considered which allow rapid periodic readout to detect any distortion in the vertical plane of the booster ring magnets.

VIII. Scheduling

For scheduling purposes the Booster II engineering and fabrication has been broken down into 26 projects. Each project leader has the additional responsibility for systematically reporting his activities. The 26 projects with their activity numbers and present milestones are shown in Fig. 17.

The scheduling is being accomplished and monitored using the program management technique of Critical Path Method (CPM).

The CPM technique is using an existing software program called Program Management System IV (PSMIV), supported by a graphics package E-2-Pert. Both programs are resident and maintained on the Applied Mathematics Division 360-195 computer. Additional information of manpower expenditure is gained by use of an ARF program called Program Planning. The manpower program provides information of the distribution of individual activities. The manpower expenditures are used as a cross reference for CPM time estimates and progress.

The reporting period for the CPM data is a calendar month, with each activity reported by the project leader. Each project leader has the responsibility to make known variances to his projected plans, in this way allowing management to act in a disciplined manner.

Early evaluation of data points to outside contract work as being of prime importance to meeting the schedule. Since all contracts have not been bid and/or let, firm times cannot be assigned. Of particular importance to the Booster II turn-on date of July 1, 1976 are the main

magnets. The construction of the magnets and their delivery have been assigned milestones 5 and 6 on the chart. At the present time these milestones have not been confirmed by the manufacturer. If these milestones are late the turn on time cannot be met; if the time is correct July 1, 1976 is attainable for turn on.

It should be emphasized that the projected turn on date is possible only because of the increased manpower which has now been placed on engineering and fabrication. At the present time, 38 physicists, engineers, and technicians have some involvement with the program.

BOOSTER II SCHEDULE

DATE: April 5, 1975

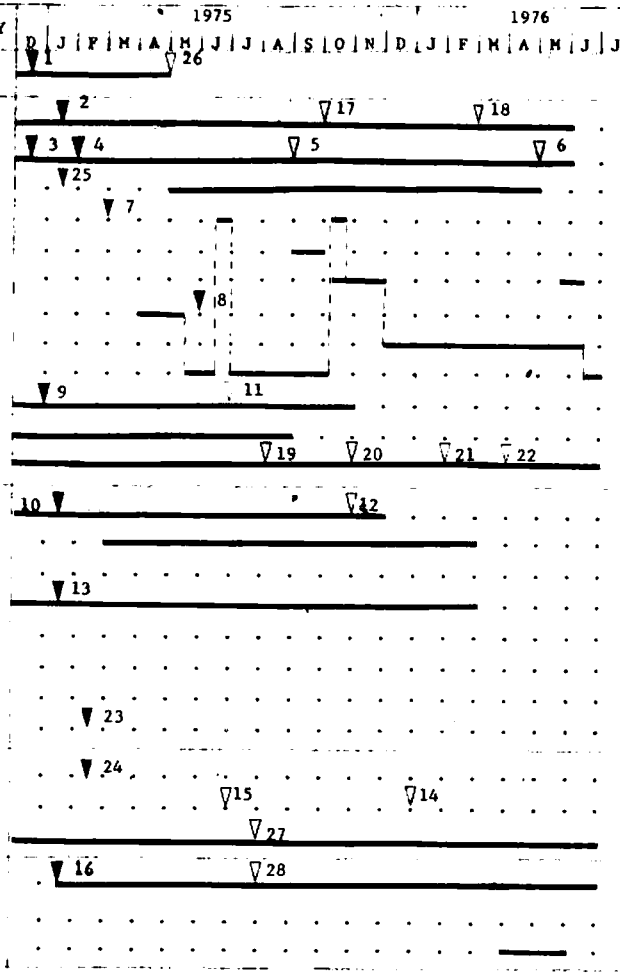

	ACTIVITY	ACTIVITY NO.	TIME TO GO	ACTIVITY NOTES
	DESIGN REPORT	B-201		Active
	R. F.	B-209		Note 1
M	MAIN MAGNETS	B-210		Note 2
A	CORRECTION MAGNETS	B-211		Active
I	SUPPORT INSTALLATION	B-220		Active
N	ALIGNMENT	B-221		Active
	SERVICES	B-230		Detailing
R	BOOSTER I REMOVAL	B-290		Note 3
I	RING INSTALLATION	B-291		Inactive
N	SHIELDING	B-292		Note 4
G	STRAIGHT SECTIONS	B-293		Active
	VACUUM	B-294		Active
	B.R.M.P.S.	B-295		Note 5
	EXTRACTION KICKER	B-240		Active
Z	EXTRACTION SEPTA	B-250		Detailing
G	500 MeV MODIFICATION	B-260		No Schedule *
S	INJECTION KICKER	B-261		Note 6
	INFLECTOR	B-262		No Schedule *
E				
X	INJECTION PROGRAM	B-264		No Schedule *
T	ZGS RIPPLE	B-265		Inactive
I	50 MeV MODIFICATION	B-270		Note 7
N	STRIPPER	B-271		Detailing
J	H⁻ SOURCE	B-272		Active
M	CONTROLS	B-280		Active
C	DIAGNOSTIC	B-281		No Schedule *
R	RADIATION SAFETY	B-282		Inactive

MILESTONES

1- Rough draft issued
26- Report issued
2- Conceptual design freeze
17- Cavity Power Tests
18- R.A. Tests
3- Fabrication bids issued
4- Fabrication contract let
5- Magnet received
6- Last magnet received
25- Conceptual design freeze
7- Test core of foundation
8- Start main ring construction critical path
9- Preliminary requirements defined
11-final review
19- P.S. Vendor Tests
20- Auto Transformer Tests
21- Choke Assembled
22- Tests P.S. with Choke
10- Ferrite contract let
12- High power tests
13- Ferrite contract let
23- Machine Research
24- Machine Research
14- Stripper modifications complete
15-Design freeze
27-N_a cell tests
16- Detailed requirements defined
28-System design complete

Note 1 The power supply is on the critical path, the 20 kV, 50 A Fermi supply is being reconditioned for possible use. The prototype cavity is ready for testing.

Note 2 Delivery schedules will be verified by June 1, this will impact B-291.

Note 3 The main ring construction path has been altered. In effect the construction of the ring and services will be complete by Dec. 1 and thus allow greater flexibility for B-291.

Note 4 The shielding effort has been increased in scope to include the 50 MeV tunnel.

Note 5 The main ring connections are being re-reviewed. The final choke configuration will be reviewed and frozen June 1.

Note 6 The injection kicker is about 2 months behind schedule due to the timing line model not being finalized.

Note 7 The general concept of 50 MeV injection has been finalized. A significant amount of detailing remains and the entire scope of the project has increased significantly.

* The absence of schedules make an accurate assessment of time and manpower difficult.